

RESEARCH



Report No. UT-20.18

ASSESSING CLOSE-RANGE PHOTOGRAMMETRY AS AN ALTERNATIVE TO LIDAR TECHNOLOGY AT UDOT DIVISIONS

Prepared For:

Utah Department of Transportation
Research & Innovation Division

**Final Report
August 2020**

DISCLAIMER

The authors alone are responsible for the preparation and accuracy of the information, data, analysis, discussions, recommendations, and conclusions presented herein. The contents do not necessarily reflect the views, opinions, endorsements, or policies of the Utah Department of Transportation or the U.S. Department of Transportation. The Utah Department of Transportation makes no representation or warranty of any kind, and assumes no liability therefore.

ACKNOWLEDGMENTS

The authors acknowledge the Utah Department of Transportation (UDOT) for funding this research, and the following individuals from UDOT on the Technical Advisory Committee for helping to guide the research:

- Vincent Liu
- Abdul Wakil
- Kaitlin Marousis
- Michael Butler
- Paul Wheeler
- Chris Whipple
- Nathan Jones
- Trevor Egan

TECHNICAL REPORT ABSTRACT

1. Report No. UT-20.18		2. Government Accession No. N/A		3. Recipient's Catalog No. N/A	
4. Title and Subtitle Assessing Close-Range Photogrammetry as an Alternative for LiDAR Technology at UDOT Divisions				5. Report Date June 2020	
				6. Performing Organization Code	
7. Author(s) Chandler Cross, Mohammad Farhadmanesh, Abbas Rashidi				8. Performing Organization Report No.	
9. Performing Organization Name and Address The University of Utah Department of Civil and Environmental Engineering 201 Presidents Circle Salt Lake City, Utah 84112				10. Work Unit No. 5H08480H	
				11. Contract or Grant No. 20-8083	
12. Sponsoring Agency Name and Address Utah Department of Transportation 4501 South 2700 West P.O. Box 148410 Salt Lake City, UT 84114-8410				13. Type of Report & Period Covered Final August 2019 to October 2020	
				14. Sponsoring Agency Code UT19.601	
15. Supplementary Notes Prepared in cooperation with the Utah Department of Transportation and the U.S. Department of Transportation, Federal Highway Administration					
16. Abstract <p>LiDAR (Light Detection and Ranging) is a mature and efficient technology currently used by various divisions of UDOT (asset management, traffic control, pavement, construction, etc.). Some of the current applications of LiDAR at UDOT (as well as other DOTs) include: asset management for roads and buildings, quality control of pavements and other infrastructure surfaces, 3D as-built documentation of constructed facilities, etc.</p> <p>While effective, there are some limitations in using LiDAR as a common engineering tool: The technology is pretty expensive, certain levels of expertise and training are required to use LiDAR scanners for data collection and processing results, and finally it might not be available for all units and individuals.</p> <p>Close-range photogrammetry is another emerging technology that could be considered as a potential alternative for LiDAR scanning devices. The technology is based on processing images and videos simply captured by off-the-shelf cameras or smartphones. Unlike LiDAR, close-range photogrammetry is very cost effective, simple, and easy-to-use. There is no need for extra hardware settings and almost everyone has a smartphone or camera so collecting and processing data is very feasible.</p> <p>Within the last decade, several software packages in the area of close-range photogrammetry have been introduced for research, education, and commercial purposes. Some examples are Autodesk Recap; Agisoft Photoscan; 3DF Zephyr; VisualSFM; and Photomodeler. The outputs of both LiDAR and Photogrammetric technologies are in the form of dense point clouds. While the output of the two methods are similar, there might be differences in level of accuracy and density of the generated point clouds. In addition, each method might work differently under certain conditions such as scanning shiny and reflective objects, sharp edges, etc.</p> <p>Despite the increasing popularity of close-range photogrammetry, it has not been considered as a practical scanning tool by UDOT divisions yet. This project aims to address this important issue by exploring the feasibility of using this technology for various applications currently handled by LiDAR at UDOT.</p>					
17. Key Words Photogrammetry, LiDAR, 3D Reconstruction			18. Distribution Statement Not restricted. Available through: UDOT Research Division 4501 South 2700 West P.O. Box 148410 Salt Lake City, UT 84114-8410 www.udot.utah.gov/go/research		23. Registrant's Seal N/A
19. Security Classification (of this report) Unclassified	20. Security Classification (of this page) Unclassified	21. 97	22. Price N/A		

TABLE OF CONTENTS

LIST OF TABLES	vi
LIST OF FIGURES	vi
UNIT CONVERSION FACTORS	ix
LIST OF ACRONYMS	x
EXECUTIVE SUMMARY	11
1.0 INTRODUCTION	12
1.1 Introduction.....	12
1.2 Problem Statement.....	14
1.3 Objectives	16
1.4 Scope.....	16
1.5 Outline of Report	17
2.0 RESEARCH METHODS	17
2.1 Background.....	17
2.1.1 Laser Scanners	17
2.1.2 Photo/Videogrammetry	19
2.1.3 Laser Scanners and Photogrammetry in Construction.....	20
2.2 Accuracy and Quality Measurement Methods.....	21
2.3 Comparison Methods	22
2.4 Summary	24
3.0 DATA COLLECTION	24
3.1 Overview.....	24
3.2 Roadway Asset Management.....	25
3.2.1 Data Acquisition Camera	25
3.2.2 Camera Settings and Mounting Procedures	29
3.2.3 LiDAR Data Collections	30
3.3 Pedestrian Access Ramp Data Collections	31
3.3.1 Pedestrian Access Ramp Inspections.....	31
3.3.2 Data Collection and Camera Settings for Image Based Reconstruction.....	32
3.3.3 LiDAR Data Collection	33

4.0 DATA EVALUATION	34
4.1 Overview.....	34
4.2 Roadway Asset Management	35
4.2.1 Accuracy assessment and Quality Assessment.....	41
4.2.2 Model 1	42
4.2.3 Model 2	44
4.2.4 Model 3	47
4.2.5 Model 4.....	50
4.2.6 Model 5	54
4.2.7 Model 6.....	57
4.3 Unmanned Aerial System Data.....	60
4.4 Pedestrian Access Ramp.....	61
4.4.1 Ramp 1	65
4.4.2 Ramp 2.....	67
4.4.3 Ramp 3	69
4.4.4 Ramp 4.....	71
4.4.5 Ramp 5.....	74
4.4.6 Ramp 6.....	74
4.5 Summary.....	75
5.0 CONCLUSIONS.....	76
5.1 Summary.....	76
5.2 Limitations and Challenges	78
6.0 RECOMMENDATIONS AND IMPLEMENTATION	80
6.1 Recommendations.....	80
6.2 Implementation Plan.....	83
6.2.1 Asset Management Implementation.....	83
6.2.2 Pedestrian Access Ramp Implementation	87
REFERENCES	89
APPENDIX A: SUPPLEMENTAL MATERIAL.....	91

LIST OF TABLES

Table 1 Comparison of Software Packages	23
Table 2 Data Collection Spreadsheet	27
Table 3 Data Collection and Processing for Pedestrian Access Ramps	33
Table 4 Data Collection and Processing for Asset Management Models.....	37
Table 5 Data Processing Table	38
Table 6 Measurement Overview for Asset Management	42
Table 7 Model 1 Sign Ratio Table	43
Table 8 Model 2 Sign Ratio Table	46
Table 9 Model 3 Sign Ratio Table	49
Table 10 Model 4 Sign Ratio Table	52
Table 11 Model 5 Sign Ratio Table	56
Table 12 Model 6 Sign Ratio Table	59
Table 13 Pedestrian Access Ramp Slope Errors.....	62
Table 14 Data Processing Table for Pedestrian Access Ramps.....	63
Table 15 Effects of Down Sampling on Point Cloud Quality	81
Table 16 Technology and Equipment Comparison	93

LIST OF FIGURES

Figure 1 Highway and Roadway Expenditures	12
Figure 2 Leica LiDAR Scanner	18
Figure 3 Mandli’s Mobile LiDAR Vehicle.....	19
Figure 4 Comparison of Various Software Packages	23
Figure 5 Hood Mounted GoPro	26
Figure 6 Different Camera Mounting Areas	30
Figure 7 Pedestrian Access Ramp Components	31
Figure 8 Smart Tool Smart Level	32
Figure 9 Slope Measurement of a Pedestrian Access Ramp	35
Figure 10 Comparison of Point Cloud Density for Model 1	44
Figure 11 Comparison of Point Cloud Density for Model 2	47
Figure 12 Comparison of Point Cloud Density for Model 3	50
Figure 13 Comparison of Point Cloud Density for Model 4	54
Figure 14 Comparison of Point Cloud Density for Model 5	57
Figure 15 Comparison of Point Cloud Density for Model 6	60
Figure 16 Comparison of UAS Point Cloud Models	61
Figure 17 Ramp 1 Point Clouds.....	65
Figure 18 Comparison Between In-Field and Point Cloud Measurements for Access Ramp 1 ...	66
Figure 19 Ramp 2 Point Clouds	67
Figure 20 Comparison Between In-Field and Point Cloud Measurements for Access Ramp 2....	68
Figure 21 Ramp 3 Point Clouds	69
Figure 22 Comparison Between In-Field and Point Cloud Measurements for Access Ramp 3....	70
Figure 23 Ramp 4 Point Clouds.....	72
Figure 24 Comparison Between In-Field and Point Cloud Measurements for Access Ramp 4....	73
Figure 25 Ramp 5 Point Clouds.....	74
Figure 26 Ramp 6 Point Clouds.....	75
Figure 27 Image Acquisition Patterns	78
Figure 28 Number of Keypoints of 3 Locations According to Acquisition Speed	80
Figure 29 Camera Mounting Area and FOV	84
Figure 30 Video Frame Extraction Window.....	84

Figure 31 Aerotriangulation Settings85
Figure 32 Maximum RAM Usage Exceeded Warning85
Figure 33 Highway Asset Management Point Cloud Using LiDAR90
Figure 34 Highway Asset Management Point Cloud Using Photogrammetry91
Figure 35 Drone Data Collection Images93
Figure 36 Keypoint Matches at Three Separate Locations93

UNIT CONVERSION FACTORS

NO UNIT CONVERSIONS

LIST OF ACRONYMS

LiDAR	Light Detection and Ranging
MUTCD	Manual on Uniform Traffic Control Devices
UDOT	Utah Department of Transportation
DOT	Department of Transportation
FOV	Field of View
CV	Coefficient of Variation
GCP	Ground Control Points
UAS	Unmanned Aerial System
TOF	Time of Flight
ADA	Americans with Disabilities Act
GSD	Ground Sampling Distance
MP	Megapixel
RGB	Red, Green, and Blue
GPS	Global Positioning System
FPS	Frames Per Second

EXECUTIVE SUMMARY

LiDAR (Light Detection and Ranging) scanners are widely used reconstruction sensors that are able to quickly capture large amounts of data and create a highly accurate virtual 3D model. More recently, image-based reconstruction known as photogrammetry has emerged in the market of 3D reconstruction as a cheaper, user-friendly alternative to the traditionally used LiDAR technologies. Currently, UDOT uses Mandli Communications to gather LiDAR data from around the state of Utah for asset management and evaluation purposes.

The purpose of this report is to detail the findings from a year-long comprehensive research study comparing LiDAR and photogrammetry technologies. Though only two technologies are being compared, there was a multitude of reconstruction instruments used such as hand-held cameras, drones equipped with cameras and LiDAR scanners, and LiDAR point clouds generated from mobile and terrestrial LiDAR scanners. The case studies mainly focused upon during this research are highway asset management, and pedestrian access ramp inspections. For each case study, point clouds were generated using LiDAR and image-based reconstruction, and then comparisons between the two clouds were carried out. These evaluations focused on variables such as point cloud density, linear accuracy, asset clarity, slopes, and overall point cloud quality. Other qualitative characteristics were evaluated as well such as cost, user interface, and ease-of-use for the average individual.

Over the course of this research study it was found that LiDAR created a more uniform and accurate point cloud, but photogrammetry also offered a high-quality point cloud that was still very accurate. Both technologies were within one percent error of each other for the asset management case study, and for the pedestrian access ramp case study there was less than 0.15 percent calculated error between LiDAR and photogrammetry technologies.

Photogrammetry is a very cost-effective way to achieve the same results as LiDAR. The research presented in this report is written to present the reader with all data that has been gathered and evaluated, as well as the findings and opinions of the researchers involved in this study. The goal of this paper is to allow the reader to have a complete understanding of how each technology works, and how each performs under various mobile and static circumstances. Due to

the different strengths and weaknesses of each technology, it is ultimately up to the user of said technology to decide which one satisfies the given requirements for the situation at hand.

1.0 INTRODUCTION

1.1 Introduction

Managers must have comprehensive data on all assets' current status to optimize the rehabilitation process in civil infrastructure facilities. Accurate asset status is necessary to monitor and be aware of the extent to which all the facilities are performing. Infrastructure in the United States consists of approximately 4,161,00 miles of roads, paved and unpaved [1], with more than 600,000 bridges, of which more than one-third are 50 years or older. According to the ASCE's Infrastructure Report Card of 2017, almost ten percent of all bridges in the United States are structurally deficient, and one out of every five miles of highway pavement is in poor condition. These statistics show that transportation infrastructure in the United States is fragile, and extreme precautionary measures are necessary in some circumstances as there is a growing backlog of transportation rehabilitation needs. There have always been debates about how to manage this extensive network of critical infrastructure properly. Monitoring the performance of assets and ensuring their maintenance is performed in a timely and satisfactory manner is of utmost importance.

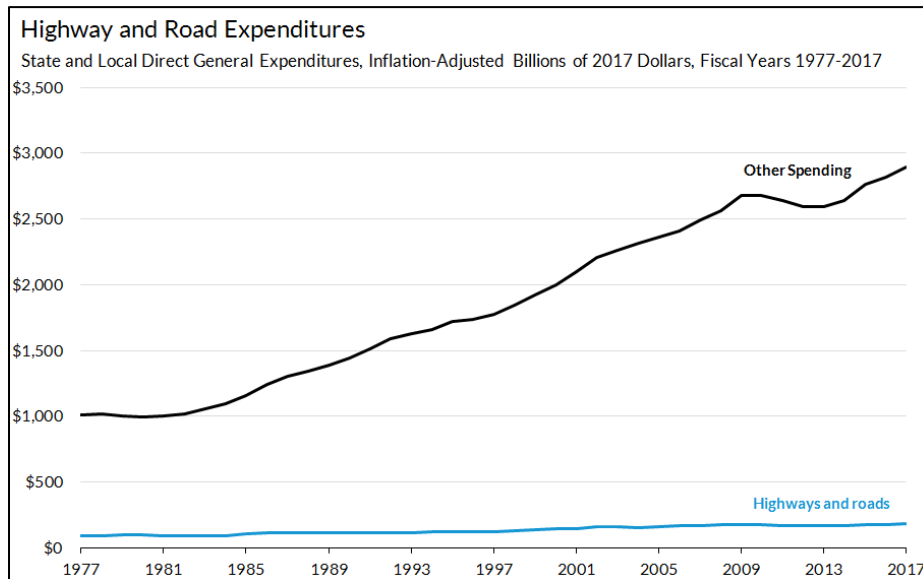


Figure 1 - Highway and Road expenditures compared to other state spending. "Highway and Road Expenditures", Urban Institute.

Many assets' life spans are affected by factors such as weathering, corrosion, installation errors, and traffic accidents. With the ever-changing state of assets, fast, reliable, and accurate monitoring procedures are needed. This problem requires an efficient data acquisition system that provides transportation departments with critical information on the current status of assets. State-of-the-art technologies are necessary for transportation departments because they are becoming increasingly more accurate, fast, and inexpensive than traditional methods. While manual vision-based data collection can provide valuable information on the status of assets, it is a time-consuming task which can lead to infrequent inspections. These gaps in inspections may lead to unreliable information on the true nature of an asset's condition. Not only are manual observations time-consuming, but they are also labor-intensive and subject to the inspector's opinions. Vision-based assessments done by a person may lead to the data being subjective and inaccurate. An accurate, comprehensive representation of all of a department's assets can help transportation facility owners make decisions based on their actual status, and it can help reduce errors due to subjective opinions and lapses in inspections. The emergence of sensing technologies (e.g., LiDAR) have allowed for civil infrastructure managers to have access to fast, accurate, and reliable data acquisition systems. Technologies such as LiDAR and photogrammetry can be a suitable alternative to manual observation-based data collections. Sensing technologies eliminate the subjectivity of manual observation-based data collection, and they also provide an accurate 3D representation of existing assets.

Time-of-flight-based LiDAR (Light Detection and Ranging) is a mature and established technology that has many uses in the fields of Civil Engineering and Construction. UDOT, along with many other DOTs, currently uses LiDAR for various applications such as asset management of roadways and buildings, quality control of pavement surfaces, and 3D as-built documentation. LiDAR technology can provide a virtual, accurate 3D model of various assets, which can be a useful tool for companies. LiDAR is helpful because it allows for creating documentation with an accurate visual model. It can allow workers to access sites or objects from their office without having to travel back into the field to collect data or measurements. While LiDAR can be an effective technology, it has limitations that might preclude it from being useful and practical as a common engineering tool. LiDAR scanners can be costly, and some scanners require specific software, which can also be expensive. Along with the expense of procuring a LiDAR scanner and software, one must have specialized training and knowledge

of the technology to operate the equipment with a high level of certainty and accuracy. In-field scanning is typically a straightforward procedure; however, post-processing can be tricky due to the software's complexity, and without the right knowledge of the software, the data may not be accurate. Finally, LiDAR may not be a viable option for many people or companies. As mentioned, it is an expensive technology, and not all people have the means to acquire the equipment and go through the necessary training.

Close-range photogrammetry is a technology similar to LiDAR, and it is emerging as a cheaper alternative to LiDAR. Photogrammetry is an image-based reconstruction technology that uses 2D images of a subject to recreate a virtual 3D model. The main benefit of using photogrammetry instead of LiDAR is that the technology is rather easy to use, and it is more cost-effective than LiDAR (Appendix A). Photogrammetry can be done with expensive drones and handheld cameras, but it can also be done with something as simple as a smartphone with a camera. There is no need for a large scanner that requires setup, leveling, and long scanning times. One captures images or videos of the point of interest and takes them back to the office for processing. There are many software packages in the world of photogrammetry that work well for research, education, and commercial purposes. A few examples of these softwares are Context Capture, 3DF Zephyr, Autodesk Recap, Agisoft Photoscan, and Visual SFM.

1.2 Problem Statement

Recently, some innovative departments of transportation (DOTs) in the United States have started making landmark decisions on the matter of implementing sensor-based data acquisition of their infrastructure. However, to that end, transportation divisions cannot sensibly choose the right technology unless they know whether that technology is able to meet their requirements or not. Due to LiDAR's promising quality on other applications, some of the pioneer DOTs in the United States have begun using LiDAR laser scanners to assist in asset documentation for maintenance purposes [2]. Although the high accuracy provided by laser scanners' point clouds has been proven, due to their astronomical prices, there has been an intense debate over the substitution of LiDAR-based reconstructed point clouds for image-based reconstructed point clouds. The accuracy and quality requirements in different transportation applications (i.e., asset management, maintenance, and structures) vary from low to high. Therefore, conducting a comparison between

the point clouds generated by laser scanners and the point clouds generated by stereo-photometry is the very measure needed in order to make an educated decision on which technology fits best. In addition, the accuracy and quality level that any sensor-based (including laser-based and photogrammetry-based) spatial data provides highly depend on all the settings in which they are collected. One important variable that governs the overall quality and accuracy of the transportation facility's data collection is the speed at which the sensor moves capturing the data. According to an extensive review of research, there is a lack of research in not only photogrammetry-based point clouds but also scanner-based point clouds taken by moving sensors (scanners and digital cameras) at different speeds. The blurry effects on the images taken by a moving camera could lead to a substantial change in the number of extracted features from the image as well as the number of matches in the pair of images. Likewise, due to being mobile during spatial data collections, even the expensive, sophisticated laser scanners cannot operate at an accuracy as high as they can in the stationary setting. Hence, the case studies have been divided into two different categories of transportation applications as follows:

- Roadway asset management and maintenance
- Pedestrian ramp inspection

The above categories have been chosen due to the different speeds of the moving sensors that are being used during the data collection. In the first category, data is collected in two sub-categories: 1. Highway (high-speed data acquisition); 2. City (low-speed data acquisition). The data for pedestrian inspection is acquired in a semi-stationary and fully-stationary setting. In addition to accuracy and quality assessment in the above categories, the cost and efficiency of the two data-acquisition approaches are evaluated as well and presented in Appendix A.

Advances in photogrammetry-based 3D reconstruction software packages have changed the way in which one can have access to the 3D representation models. The previously open-sourced programs are now available through these software packages in a compacted version, which is easier to use for non-expert users. Still, according to their different algorithms in processing and providing the final output, non-expert users need guidance in choosing the software package that is suitable to their application. According to the challenges of data acquisition in the transportation area, the sensitivity of the images during processing can be very high. That is why different

software packages were used on the same data, to study their feasibility in the above-mentioned transportation applications.

In addition, these fast-prepared 3D representations could also help project managers to document the existing assets on their sites. Thus, in this paper, a realistic assessment of the time needed for data collection and data processing for each of the different mentioned tasks has been included. This is to help decision-makers when it comes to deciding to employ one of these technologies in their projects.

While the accuracy of these remote sensing techniques is highly sensitive to harsh weather and environmental conditions, investigating the quality and ability of these techniques in conditions such as rainy, snowy, and stormy days, which highly affect the reflectivity of surfaces, are outside the scope of this research. Nevertheless, the influence of different lighting conditions in outdoor settings is explored in this research.

1.3 Objectives

LiDAR and photogrammetry output processed data in the form of 3D point clouds. While the output is similar for both technologies, parameters such as the density of generated point clouds and levels of accuracy may differ. Also, one technology may work better than the other depending on environmental conditions and the distance of the object/site of interest. Despite the growing popularity of close-range photogrammetry and its ease of use and low-cost technology, it has not yet been considered a practical scanning tool within UDOT divisions. The purpose of this project and report is to address this issue and explore the feasibility of using close-range photogrammetry as an alternative technology to the currently used LiDAR technology at UDOT.

1.4 Scope

The scope of this project covers a few different divisions within the transportation department in order to have a comprehensive data set that covers multiple disciplines. The scope of work of this research covers the following:

- Highway/City Road Asset Management and Inspections
- Pedestrian Access Ramp Inspections

The reason research was conducted in these two areas is because each case requires a different data acquisition approach, and data is analyzed differently within each discipline. Asset management data acquisition is done in a completely mobile state which makes it different from pedestrian-access-ramp data acquisitions. Due to the mobile nature of data acquisitions for asset management and the speed being traveled, point cloud data can be subject to higher errors, therefore it was important to have other research areas to conduct studies in a semi-static data collection procedure. In each case, reconstructed data is analyzed differently to see how photogrammetry would perform compared to standard LiDAR procedures.

1.5 Outline of Report

- Introduction
- Research Methods
- Data Collection
- Data Evaluation
- Conclusions
- Recommendations and Implementation

2.0 RESEARCH METHODS

2.1 Background

2.1.1 Laser Scanners

LiDAR is an established technology that is continuing to grow and be proven as a useful tool to a multitude of industries. There are three main types of laser scanning technologies; time-of-flight (TOF), phase shift, and triangulation-based systems. Phase shift scanners tend to be the fastest data acquisition system; however, they have a limited range of around 80 meters.

Triangulation-based scanners are limited to a range of less than 5 meters, which makes them suitable for scanning small objects at a close range. Most long-range scanning is performed by a TOF LiDAR scanner because they have the greatest data acquisition range, reaching up to hundreds of meters. However, the long range of these scanners can cause longer data acquisition times and lower accuracy. TOF scanners operate by sending out a laser pulse which is then reflected from a given surface and returns to the scanner's sensor. The sensor uses the time of flight of the pulse and the speed of light to accurately calculate the distance traveled. The differences in laser return times and changes of laser wavelengths are used together to make a precise virtual representation of a surface and its individual characteristics. Each pulse stores information such as spatial coordinates, RGB data, and intensity data. Over the course of scanning an object or site, this data is organized and stored in points that collectively create the overall point cloud. Quite a few studies have been carried out to evaluate the performance [3], accuracy [4], and quality of laser scanners on generating spatial data from different scenes [5] with various surfaces [6] in different lighting and ambient conditions [7]. Even the first models of laser scanners held the promise of giving a high-definition output (in increments of one millimeter) at ranges from 1.5 m to 50 m in an indoor setting [4]. Furthermore, some studies on the generated point clouds of different surfaces show a slight reduction in accuracy of LiDAR technology while scanning dark [5] and wet surfaces [6].



[Figure 2 - Leica LiDAR Scanner. "Leica RTC360", Spatial Technologies.](#)

In practice, laser scanners have been employed for transportation applications such as: 1. Urban modeling; 2. Asset inventory; 2. Intersection modeling; 3. Asset encroachment collection; 4.

Overhead clearance measurements of obstructions in roadways; 5. Acquisition of pavement condition data.



Figure 3 – Mandli’s Mobile LiDAR Vehicle

2.1.2 Photo/Videogrammetry

Image-based 3D reconstruction is the process of taking 2D images from 3D objects, and then processing the images to create a 3D point cloud. In this method, spatial information of an object is obtained from a set of photos and/or video frames. The summarized process is as follows: 1. Image acquisition: Two or more images are needed for every single point in the real world to be reconstructed. Later, the acquired views of the point in the scene will go through the triangulation process; 2. Feature extraction: Points with distinguished features (such as corners) are detected to computationally characterize the acquired images; 3. Camera calibration and image registration: In order to estimate the position and orientation of the cameras in the world coordinate, detected features in multiple photos are utilized to find intrinsic and extrinsic camera parameters; 4. Depth determination: Finally, correspondences are found by feature-matching between pairs of images to determine the depth information of the points in the 2D images into the 3D space using the triangulation process.

Similar to LiDAR technology, feasibility studies on image-based 3D reconstruction are carried out in transportation, construction, and structure-related applications [8]. Despite their lower accuracy in comparison to LiDAR technology [9], image-based as-built 3D reconstruction of civil infrastructures [10] [11] as well as photogrammetry-based construction project progress monitoring are among the most established applications in the civil engineering area. Klein et al.

[11] worked on environmental limitations (occlusions by labor, construction machinery, etc.) of image-based as-built documentation of buildings on construction sites.

The only difference between photogrammetry and videogrammetry is that instead of images, video frames are processed to measure and obtain spatial data. However, according to the lower resolution of the video frames compared to the digital images, studies focusing on videogrammetry have been conducted. Pollefeys et al. [12] made use of video in order to reconstruct 3D models of urban areas in a real-time manner. Brilakis et al. [13] presented a framework in data acquisition by videogrammetry. Additionally, an optimized selection of the keyframes method is given by Rashidi et al. [14] in order to make the most of the collected video data.

2.1.3 Laser Scanners and Photogrammetry in Construction

LiDAR Technology dates back to the 1960s, however it was not utilized as a tool in design and engineering until the 1990s. Budget optimization and data management is pivotal in having a successful and profitable construction project. It is important to be able to collect and recall important information quickly during various phases of construction. Laser scanning and photogrammetry have emerged as a solution that makes planning, construction, and phase monitoring easier and faster. The information provided by these technologies provides immediate and accurate measurements that can be used for precise project coordination. Laser scanners can gather quality information much faster than conventional project mapping. Tasks that may require hours or days of inspection by an individual manually can be completed in minutes by a scanner. Cost saving in construction is of utmost importance, and saving time tends to save money. Not only do LiDAR and photogrammetry save time, but they reduce tedious manual labor. When inspection or mapping is carried out by an individual who is fatigued from manual labor, the measurements may be prone to error. Scanning can help reduce error and ensure a higher level of accuracy. Incorporating these technologies into a construction workplace may also help streamline coordination. Having an accurate 3D model in the form of a point cloud allows for workers to share files and extract precise information without having to travel back into the field to do so. Valuable information can be shared effortlessly between parties.

There is a vast amount of research online that helps prove that these technologies can offer many advantages in construction over conventional procedures. Lato et al. [15] conducted a study into the mapping of shotcrete thickness using LiDAR and photogrammetry. Lato used this data to correct over-calculations of shotcrete due to rockmass convergence. Veneziano et al. [16] noticed the need for quick and accurate information regarding surface terrain during construction or relocation of infrastructure facilities and quickly turned to LiDAR and photogrammetry as a promising alternative. Veneziano et al. utilized LiDAR in conjunction with photogrammetric mapping to speed up construction phases to save time and money. A common finding in many research studies is that LiDAR and photogrammetry can be a tremendous help in cutting project costs and lost time. There is an initial upfront cost with these technologies, however the jobs that can be done with them tend to be much faster and more accurate than traditional manual procedures. Both technologies are proving to be promising tools in construction and engineering and are quickly on their way to becoming standard in the industry.

2.2 Accuracy and Quality Measurement Methods

In order to quantitatively characterize the quality of the point clouds resulted by both ultra-light laser scanners and digital cameras, different procedures and measurements have been improvised for each category (roadway asset management and maintenance, and pedestrian ramp inspection).

Linear accuracy evaluation is carried out by comparison of the ratios of length to width [17] in different planar objects. Subsequently, the actual ratios and the ratios obtained from the 3D models are compared to each other to find the error in reconstructing those planar objects. To follow a standard method for measuring the length of planar objects' sides, using the KD-tree algorithm, which is based on a space-partitioning data structure [18], a planar facet is superimposed on the surface of interest such as traffic signs' point clouds and pavement point clouds. Cartesian distances of two ends of each side (edge) on the detected, usually rectangular, surfaces by KD-tree fusion are considered as the length of that side. In this way, subjective measurements decrease significantly since picking the endpoints of an edge in a point cloud can be varied to some extent person by person. Since the superimposed surfaces on rectangular shapes

in the point cloud (traffic signs, strips, etc.) are not always a perfect rectangle, there is still some error in this measurement in some cases; however, this error is very low and negligible. The computed errors are subjected to +-1% error.

Based on the geometry, the slope of a line in the 3D space of the generated point clouds is calculated by dividing the rise by run. With the z-axis aligned with the elevation (rise) axis, slope calculation is simply calculated as follows:

$$\begin{aligned}\text{Slope} &= \frac{\text{rise}}{\text{run}} \\ \text{rise} &= \Delta z \\ \text{run} &= \sqrt{\Delta x^2 + \Delta y^2}\end{aligned}$$

Quality assessment of the completeness is carried out by comparison of the spatial data resolution in the generated point clouds. To that end, the number of points around each point within a certain radius in the point cloud are counted in order to determine the density distribution. Saturation of the point clouds is determined by counting the number of points with the same nearest-neighbor distances. For further illustration, a histogram of both the density distribution and the saturation is made.

2.3 Comparison Methods

Point clouds are compared in 1. Accuracy; 2. Spatial data resolution; 3. Operation time: day; 4. Software cost; 5. Equipment cost; 6. Data-acquisition time; 7. Data-acquisition surveyor and labor cost: (number of labors and/or surveyor needed) 8. Data processing time; 9. Difficulty level of the techniques; 10. Portability of the data; 11. Ease of transferring the technology to the second users; 12. Measurement range of distance; 13. Data storage requirement.

As previously mentioned, there is a vast array of software packages that can be used for image-based 3D reconstruction. However, most of those softwares are geared towards semi-static or drone data acquisition in which the sensor captures data in a circular pattern around the object of interest. For the asset management portion of this project, decisions needed to be made about which software package would work best in this case due to the linear nature of data acquisitions. This was done by using a control set of 163 images that were captured during data acquisition of a city street (Table 1). The same 163 images were uploaded into each software package, and

variables such as registered images, processing time, number of points, and overall point cloud quality were evaluated [Table 1]. It is of utmost importance to choose the software packages that provide a dense point cloud output and clear enough data. After reviewing the data output from each software package, the conclusion was reached that for the asset management portion of this research, Context Capture and 3DF Zephyr provided the most comprehensive and complete point clouds (Figure 4, a-e).

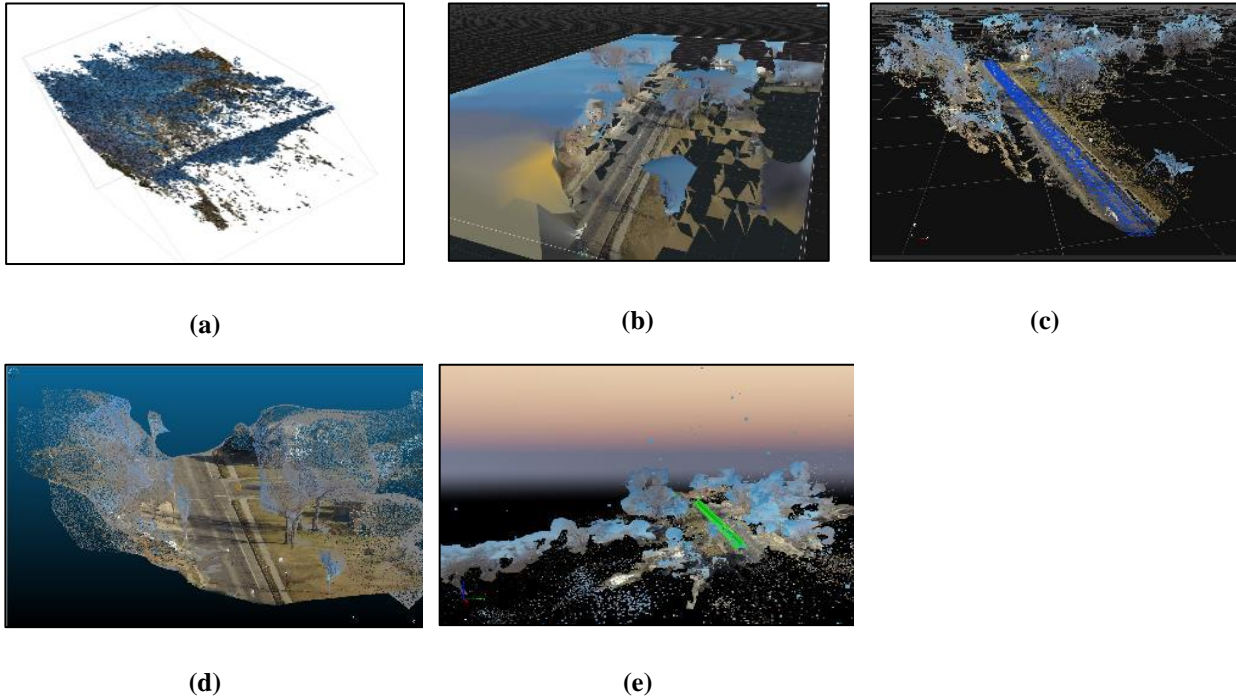


Figure 4 - Comparison of various software packages using the same control set of 163 images. (a) Agisoft, (b) Reality Capture, (c) 3DF Zephyr, (d) Context Capture, (e) Pix4D

Table 1 – Comparison of different software packages using a control set of 163 images

Software Package	Number of Registered Images (Out of 163)	Processing Time (hrs)	Number of Generated Points	Point Cloud Quality
Agisoft	89	3.5	21,145,499	Terrible
Reality Capture	161	3	12,000,000	Poor
3DF Zephyr	163	2	2,102,289	Good
Context Capture	163	1.75	55,104,235	Great
Pix 4D	163	4	1,452,751	Poor

2.4 Summary

Image-based and LiDAR-based reconstruction have a role to play when it comes to asset management and evaluations in the world of transportation. Both technologies have positive and negative characteristics, therefore the purpose of this research study is to carry out comprehensive comparisons between the two technologies by implementing them in two very different asset management applications. By applying these technologies throughout areas such as highway transportation asset management and ADA pedestrian access ramps, a conclusion can be drawn on which technology works best in the situations at hand. Variables such as density, linear accuracy, and slope measurements can be used to see how each technology will perform, and in which environment each technology thrives. Not only will the performance of each technology be evaluated, but cost and the overall ease-of-use of the technologies and corresponding softwares will also be included in the evaluations.

3.0 DATA COLLECTION

3.1 Overview

Data collections for this research project were done in varying settings with different data acquisition cameras. Asset Management data collections were carried out in a fully mobile data collection procedure using a small high-quality action-sports camera mounted to the hood of a vehicle while traveling down highways and city streets. In image-based reconstruction, it is recommended that the camera operator travel around the object of interest in a circular pattern while taking pictures in order to have sufficient overlap between images of all sides of the object of interest. This collection procedure was simply not possible due to the linear nature of highway and city roads, therefore different settings and programs were tested to see which would work best. A trial-and-error procedure using various camera settings, camera angles, and mounting positions were tested during this data collection portion to gauge which would provide the best data, and they are discussed further along in this section.

Data collections for pedestrian access ramps are much different than the collections done for asset management, and they are done in a more traditional manner. The first step in the pedestrian access ramp collection was setting up a meeting with the access ramp professionals

from UDOT to get a better understanding of what a pedestrian ramp is and the various components that it is comprised of. After this meeting, a handheld camera was used to capture images from all sides and angles of a pedestrian access ramp, and those images were later processed using a 3D reconstruction software. While the data collection procedures for each study are quite different, point cloud models were able to be generated using both linear and traditional data collection methods.

3.2 Roadway Asset Management

3.2.1 Data Acquisition Cameras

Data collection for the asset management portion of this project included testing a number of different camera settings, traveling speeds, lighting conditions, and directions of travel. Initially, data collection started on city streets due to the ability to find sections of road that have limited traffic and lower speed limits. It was important to test different software, processing settings, and camera settings to fine-tune the collection procedures before moving on to an area that requires a high-speed data collection such as a highway.

Data collections were carried out by mounting a GoPro camera to various areas of a Toyota Tacoma using a suction cup mount [Figure 5]. The initial camera used for data collections was a GoPro Hero 3+ Black Edition. This was a good camera to start with, however it is limited to 4k video resolution at 15 frames per second, and 2.7k video resolution at 30 frames per second. Another downfall of this camera is the lack of in-camera video stabilization. It is imperative to have a stabilized video when traveling at highway speeds in order for the extracted video frames to be clear and not blurry. After honing in the collection procedures and ensuring good roadway models were attainable, the decision was made to purchase the new GoPro Hero 8 camera to carry out the rest of the asset management data collection procedures. Both cameras have a 12-megapixel sensor, however this camera far surpasses the GoPro Hero 3+ with video resolutions such as 4k resolution at 60 frames per second, 2.7k resolution at 120 frames per second, and 1080P resolution at 240 frames per second. Along with the improved resolution to frame rate of this camera, it has great in-body video stabilization which makes each video extremely smooth and clear, even traveling at highway speeds. Along with using a GoPro, a DJI

Mavic Pro 2 was used to carry out UAS data collections. These collections were done with the supervision of Paul Wheeler from the UDOT Aeronautics division. During data collections the image overlap was set to 80% between each image, and each image has a precision of 1.03 inch/pixel ground sampling distance (GSD).



Figure 5 – GoPro mounted to hood of vehicle using suction cup mount

Data was collected from a multitude of roads that vary in speed, traffic conditions, assets, and pavement markings [Table 2]. Not all data collections are documented in the referenced table because of factors such as bad video quality, too much traffic to collect data, or the data just was not good enough to process an acceptable model. The table shows the data collection runs that were pivotal in these research efforts. After successfully creating a good city street model with the new GoPro camera, work began on the most important part of the asset management portion of this project, which is highways. Highways were initially a bit of trouble because rather than traveling at 25 miles per hour with limited traffic, speeds were anywhere from 40-60 miles per hour during collection with a large amount of traffic and fast-moving vehicles.

Table 2 – Data Collection Spreadsheet

Date & Time	Comments about collection	Road Location	Miles Driven During Data Collection	Driving Direction (N,S,E,W)	Recording Settings	Speed Limit (MPH)	Actual Speed (MPH)	Road Condition	Camera Position	Angles (0° is straight forward)	Sky Conditions
11/8/2020 1:00 PM	City Street data collection to work on asset management	on 700W just off of 1700S	6 Miles	South	2.7K @ 30 FPS, Wide	25	25	Asphalt, lots of black streaks from assumed crack repairs	Centered on hood	0°	Sunny
11/18/2019 12:00PM	City Street data collection to work on asset management	On 600W just off of 1700S	8 Miles	North	2.7K @ 30 FPS, Wide	30	25	Asphalt road	Centered on hood	0°	Sunny
1/14/2020, 12:45 PM	City Street data collection to work on asset management	1300 S Between 900E and Lincoln Street	12 Miles	East	2.7K @ 30 FPS, Wide	30	25	Asphalt, lots of black streaks from assumed crack repairs	Centered on hood	0°	Sunny
2/08/2020, 1:45 PM	City Street data collection to work on asset management	Driving North on 900W between 1700S and 1300S	5 Miles	North	2.7K @ 30 FPS, Wide	30	25	The road appeared to be asphalt but had sections of road repairs	Centered on hood	0°	Partly Cloudy with blue skies
2/11/2020, 2:00 PM	City Street data collection to work on asset management	1300 S between 700E and 1100E	8 Miles	East	4K @ 30 FPS, Linear	30	30	Asphalt, lots of black streaks from assumed crack repairs	Centered on hood	0°	Mostly cloud covered. Still good illumination
2/14/2020 1:00PM	Highway collection	I-15N	18 Miles	North	2.7k @ 120 FPS, Linear	70	60	typical highway	Centered on hood	0°	Light cloud cover with good sunlight
2/17/2020, 2:00 PM	I was focusing on pavement for this collection.	1301 S between 700E and 1100E	8 Miles	East	4K @ 30 FPS, Linear	30	30	Asphalt, lots of black streaks from assumed crack repairs	Centered on hood	0°	Light cloud cover with good sunlight
2/19/2020, 12:00PM	I found a location that I thought may be good to process so I ran through this particular section of I-15N a few times to try to get some acceptable data	I-15N	25 Miles	North	2.7K @ 120, Wide	65	60	typical highway	Centered on hood	0°	No clouds. Sunny
2/19/2020, 2:00PM	Trying to collect videos from various areas of I-215N	I-215N	23 Miles	West	1080P @ 120, Linear	65	60	typical highway	Centered on hood	0°	No clouds. Sunny
2/20/2020, 11:00 AM	Trying to collect videos from I-15N in various locations	I-15N	17 Miles	North	2.7k @ 60 FPS, Linear	65	~60	typical highway	Centered on hood	0°	Light cloud cover with good sunlight
2/20/2020, 11:00 AM	Trying to collect videos from I-15N in various locations	I-15N	19 Miles	North	4k @ 60, Wide	65	60	typical highway	Centered on hood	0°	No clouds. Sunny
2/21/2020, 2:00 PM	This particular run I decided to try a different approach to data collections. I tried to use 3 different camera angles, one facing left by 15 degrees, one centered, and one facing right by 15 degrees. I did this to see if we could merge all videos in context capture	I-201 East	15 Miles	East	2.7K @ 60, linear	65	60-65	rough highway with ongoing construction	one view left, one center, one right	- 15°,0°,15°	No clouds. Sunny
2/23/2020, 3:00 PM	Trying to collect videos from I-15N in various locations	I-15N	25 Miles	North	4K @ 30 FPS, Linear	65	55	typical highway	one view left, one center, one right	- 10°,0°,10°	Very little clouds

Table 2 cont. – Data Collection Spreadsheet

3/15/2020, 9:45 AM	This day I was recording videos from a specific section of I-15N that I knew had less vehicle traffic and I could drive slower	I-15N	14 Miles	North	1 run with 4K @ 60 FPS and 2 runs with 2.7K @ 120 FPS	65	45-55	typical highway	Centered on hood	0°	Very little clouds
3/15/2020, 11 AM	Trying to collect data from the first portion of mandli's model	I-15N	12 Miles	North	2.7k @ 120 FPS, wide	65	55-60	typical highway	Centered on hood	0°	No clouds
3/23/3030, 10:45:00 AM	Trying to collect more videos from section 1 since the previous section 1 model was not the best. Tried to drive slower	I-15N	10 Miles	North	2.7K @ 120 FPS, wide	65	55	typical highway	Centered on hood	0°	Cloudy, storm moving in, low sunlight
3/24/2020, 11:00 AM	This video was to collect data on the last portion of the model we had from mandli	I-15N Exit	6 Miles	North then South	2.7K @ 120, Wide	25	20	typical highway	Centered on hood	0°	Cloudy, low sunlight
4/28/2019 5:30 PM	The purpose of this data collection was to record videos from a different highway than I-15. I recorded various videos from all over I-80 driving east.	I-80E	23 Miles	East	2.7K @ 120, Wide	65	50	typical highway	Centered on hood	0°	No clouds
5/9/2020 11:00 AM	This collections purpose was to record the same section using 6 different video resolutions to try to compare the outcomes of various video resolutions	Driving north on I-15. All videos were recorded on what is previously known as "section 2"	34 Miles	North	4k@60 FPS, Wide 4k@60, Linear 2.7K @ 60, Linear 2.7K @ 120, Wide 1080 @ 240, Wide 1080 @ 120, Linear	60	45-50	typical highway	Centered on hood	0°	No clouds
5/17/2020 2:00PM	The purpose of this collection was to try to collect much data as possible. It was a cloudy day so I wanted to collect data from "section 2" in order to compare it to the section 2 from a sunny day. I also tried to get videos from a new highway (201) and I also tried to get videos from a 1 mile long section. Today wasnt the best day though because it was pretty busy and I was not really able to drive below 50 MPH. I got down to 40 on section 2	Driving North and south on I-15, driving east on I-80, driving east and west on 201	44 miles	North, South, East, West	2.7k @ 120, Wide	65-70	50-55	typical highway	Centered on hood	0°	Cloud coverage, low sunlight
5/27/2020 1:00PM	The purpose of this data collection was to collect videos from different speeds of a small section of road. The first speed was less than 10MPH, then 10,20,30,40MPH. It was a nice sunny day with a little bit of cloud cover	Driving North on a city street	6 miles	North	2.7k @ 120, Wide	25	<10,10,20,30,40	City street with lots of repairs	Centered on hood	0°	No cloud cover

3.2.2 Camera Settings and Mounting Procedures

Numerous variations of camera resolutions and frame rates were tested to figure out which settings are optimal for highway data collections. Out of all of the settings and combinations, the combination that worked best and provided the best point cloud model is 2.7k resolution at 120 frames per second with a wide field of view (FOV). The GoPro camera offers FOV's such as linear, wide, and super-view. The linear FOV did not capture enough data regarding the signs that line the sides of the highway, and the super-view FOV was far too wide and stretched to create a reasonable model. The wide FOV captured signs on the sides of the highway road with limited video and model distortion.

Along with testing resolution and frame rate combinations, different camera mounting angles and heights were also tested. There was also the question of whether mounting the camera on the hood of the vehicle or on the roof of the vehicle would work better for data collection. After evaluating data regarding both cases, a camera mounted on the hood worked much better than a camera mounted on the roof of the vehicle. When the camera is mounted on the roof of the vehicle as shown in Figure 6 (b), it is difficult to angle the camera in a way such that the hood of the vehicle is not in the field of view. If the camera is angled too far up excluding the hood from the field of view, the camera will not capture enough data on the pavement of the road and signs lower on the roadway. If the camera is angled too low on the roof of the vehicle, the hood of the vehicle will be in the field of view of the camera which can cause errors during processing [Figure 6 (d)]. A hood-mounted camera was easy to angle in a way such that the entire roadway and all pertinent signs are in the field of view, all while omitting parts of the vehicle from the video [Figure 6 (a) and (c)]. Along with different mounting elevations/locations, multiple camera viewing angles were tested. Three iterations would be completed over one section of highway road: One with the camera facing straight forward, one with the camera rotated about fifteen degrees to the left, and another with the camera rotated about fifteen degrees to the right. Frames were then extracted from each video, and then images were submitted for alignment. However, a camera mounted straight forward tended to provide best video and overall point cloud models.



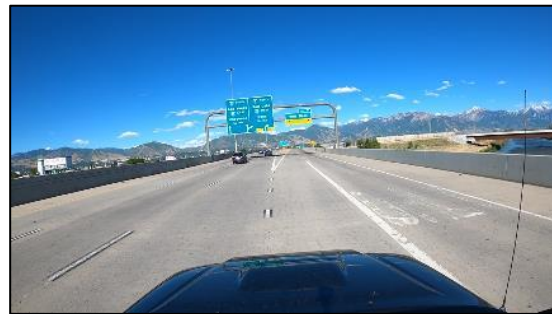
(a)



(b)



(c)



(d)

Figure 6 – Different mounting areas and their corresponding view. (a) Camera mounted on hood, (b) camera mounted on roof, (c) Field of view of hood-mounted camera, (d) Field of view of roof-mounted camera

3.2.3 LiDAR Data Collections

LiDAR data was collected by Mandli while under contract with UDOT. LiDAR models were obtained from connections within UDOT in order to carry out the comparisons between point clouds. LiDAR models were obtained for each successful highway model that was generated. Along with obtaining Mandli's mobile LiDAR data, during the same meeting with Paul Wheeler, a DJI M600 drone with a mounted VX15 LiDAR scanner was used to gather highway data. This LiDAR scanner is able to capture up to 100,000 points per second.

3.3 Pedestrian Access Ramp Data Collections

3.3.1 Pedestrian Access Ramp Inspections

Data for the pedestrian access ramp portion of this project was collected from multiple locations with varying types of pedestrian access ramps to have a wide variety of point clouds to study. The first step in the pedestrian access ramp portion was to meet with UDOT and get a general idea of the different components of an access ramp, and get an idea of the type of measurements and inspections that are done in the field. Upon meeting with UDOT representatives in the office, a date was set to meet in the field and carry out the inspections of four pedestrian access ramps according to standard procedures outlined in the UDOT C-170 Pedestrian Access Ramp Evaluation form. This meeting was imperative, as there are many different components to an access ramp [Figure 7], each of which has different measurement requirements and specifications.

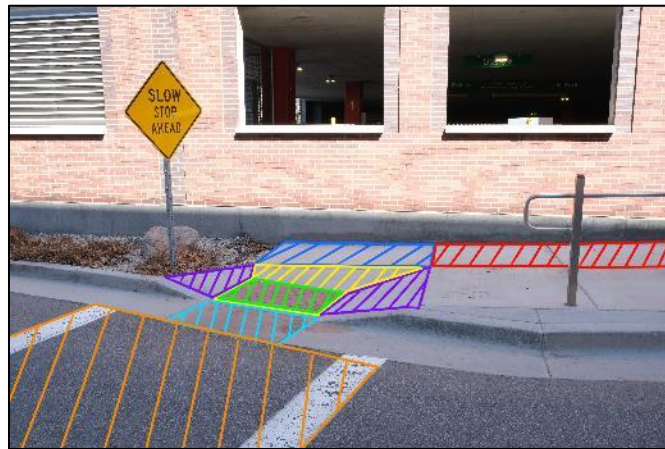


Figure 7 – Pedestrian Access Ramp Components. Red: Pedestrian Access Route (PAR); Blue: Turning Space (T); Yellow: Ramp; Purple: Flares; Green: Detectable Warning Surface (DWS); Light Blue: Clear Space; Orange: Crosswalk

The inspections done by UDOT were carried out using a Smart Tool Smart Level [Figure 8], and a tape measure. The Smart Tool was used to measure the slope percentages of the various ramp components to ensure they were within the specified requirements, and the tape measure was used to ensure that various widths and distances of the ramp are also within

requirements. Upon completing the inspections with the representatives of UDOT, we were able to keep the inspection reports from each ramp inspection, that way in-field inspection measurements could be evaluated while extracting point cloud measurements.



[Figure 8 – Smart Tool Smart level](#)

3.3.2 Data Collection and Camera Settings for Image-Based Reconstruction

For the image-based portion of the pedestrian access ramp project, images were collected in a semi-static procedure that encompasses the entire access ramp area. The camera used for data collection was a Fujifilm XT-30 mirrorless digital camera. The Fujifilm XT-30 has a large 26.1 MP sensor capable of capturing high-quality images with a lot of data in each image. The procedure for collecting data on each access ramp includes moving in a circle around the access ramp in question. It is important to be far enough away from the access ramp to capture all pertinent components, but not so far that it's difficult for the camera to collect enough detail on all components. It is also imperative to move in a circular pattern around the access ramp because each image must have a large amount of overlap for the processing software to successfully align images. Each pedestrian ramp was generated using around 30 images, some needed more images and some needed less depending on how large the pedestrian access ramp is. There needed to be a delicate balance between collecting enough detail of each ramp while ensuring there was not an unnecessary number of images. If too many images are used, the point cloud density may be higher, however the file size can be very large and may cause programs to run slow. For this portion of research, the point clouds do not need to have a high number of images and an extreme density. A clean, comprehensive point cloud with acceptable point density and distinct enough features for evaluation can be achieved as long as there is sufficient overlap between images, meaning that each point in the scene must be captured in at least three

different images with different viewing angles. It is vital to ensure that all procedures are carried out in a way such that data size is optimal for processing and transferring between parties.

3.3.3 LiDAR Data Collection

The LiDAR portion of this case study was carried out using a Maptek I-Site 8820 terrestrial LiDAR scanner. This particular scanner is a long-range laser scanner capable of reaching distances of up to 2,000 meters. The laser scanner also has built-in panoramic imaging to give point clouds an accurate RGB color representation. The user also has many customizable settings that can be adjusted for different scanner scenarios such as: lighting conditions, point cloud density, image capture, and necessary accuracy. Setup and use of this laser scanner are quick and easy processes that include leveling the scanner, inputting the appropriate settings for the given scenario, and beginning scanning. Once the user starts the scanning process, the laser scanner does the rest of the work. Along with the scanner body, the laser scanner comes with a Panasonic tablet that allows for an easy streamlined scanning process, and gives the user the option to preview the scanning area to ensure that all necessary elements in the scene are captured. Table 3 below shows the data collection times, processing times, and a general overview of the point clouds created.

Table 3 – Data collection and processing for pedestrian access ramps using photogrammetry and LiDAR

Method	Model	In-Field Data Acquisition Time (Minutes)	Number of images/scans (Aligned/Total)	Processing Time	Number of Points in Point Cloud	File Size
Image-based Reconstruction	Ramp 1	< 5 min	31/31	47 min 2 sec	258,651,814	6.72 GB
	Ramp 2	< 5 min	37/37	52 min 22 sec	429,797,343	11.17 GB
	Ramp 3	< 5 min	27/29	52 min 26 sec	313,767,481	8.16 GB
	Ramp 4	< 5 min	31/31	47 min 8 sec	263,338,208	6.87 GB
	Ramp 5	< 5 min	27/29	51 min 23 sec	436,552,997	11.35 GB
	Ramp 6	< 5 min	24/25	49 min 20 sec	247,958,617	6.45 GB
LiDAR-Based Reconstruction	Ramp 1	16 m 30 s	1 scan	No Processing	12,182,400	768 MB
	Ramp 2	17 min	1 scan	No Processing	11,955,200	745 MB
	Ramp 3	12 m 9 s	1 scan	No Processing	3,498,634	222 MB
	Ramp 4	13 m 45 s	1 scan	No Processing	6,506,448	407 MB
	Ramp 5	13 m 9 s	1 scan	No Processing	2,999,779	102 MB
	Ramp 6	13 m 32 s	1 scan	No Processing	2,398,708	83 MB

4.0 DATA EVALUATION

4.1 Overview

Data evaluations were done separately for each case in this research project, however some of the principles are the same for each. For the asset management portion, models were compared in different ways. The first was comparing the overall density of point cloud models using multiple density algorithms, but the most important density variable is the number of neighbors. This is calculated by defining the radius of a sphere, and then the program calculates the number of points within a sphere with that radius. These spheres are imposed throughout the point cloud to get an overall index of uniformity. An equivalent radius of one centimeter was used. The reason an equivalent radius is necessary is because both the photogrammetry model and LiDAR model are in arbitrary units. Ground control points with known GPS coordinates are necessary in order to have a model with a scale accurate to the real world. However, ground control points are difficult to input into the model due to the location of data collections. It would be difficult to go onto the highway to get known GPS coordinates of particular points. The equivalent radius was calculated by extracting a measurement from the point cloud (e.g., width of a sign), and then comparing that measurement to the actual measurement in real life to obtain the scale of the model. Histograms and point cloud saturation images are included further along in this section. Along with the density of point clouds, accuracy of the size of reconstructed elements (e.g., signs) was also evaluated by comparing the ratios (height to width) of generated signs to the actual ratios of the signs in real life. Measurements were extracted from the image-based point cloud and the LiDAR point cloud and then compared to the actual sign ratios to calculate a relative error.

Data for the pedestrian access ramps was evaluated in ways that are similar to the evaluations of asset management point clouds. First, the density of point cloud models was calculated in the same way as the density for asset management point clouds, using the number of neighbors index. One of the most important measurements that are recorded from access ramp inspections are the slopes of various areas of the ramp. As mentioned previously, the ramps are made up of multiple components, and each component has slightly different slope and distance requirements. The accuracy of extracted slope measurements was evaluated from point clouds

along with the density readings to see if the slopes extracted from the point clouds were similar to slopes extracted from the in-field inspections. Slopes were measured in the point clouds by picking two points on the surface of the ramp component in question, and then dividing the change in Z coordinates by the distance of the projection along the XY plane [Figure 9].



Figure 9 – Slope measurement of a flare component of a pedestrian access ramp. ΔZ is the change in elevation, ΔXY is the projected distance along the XY plane.

4.2. Roadway Asset Management

Data evaluation of the reconstructed roadway point clouds is imperative to gauge whether or not photogrammetry technology would provide sufficient enough data to be comparable to traditional LiDAR procedures. Table 4 below shows the data acquisition and processing time for all models from this case study. In the following data processing table [Table 5], you will see all of the information used to track the data collections, camera information, and processing information. Some data collections were processed multiple times, which explains why the data processing table may not match up exactly to the data collection table. During data collections, numerous videos are taken and may be processed at different times. Overall, the photogrammetry point clouds that were produced were very comparable to the provided LiDAR point clouds in terms of density and relative errors. One important factor to note is that in the following pages there will be images showing the densities of point clouds generated by photogrammetry and

point clouds generated by LiDAR. In each case, the photogrammetry point cloud is much denser than the LiDAR point clouds. LiDAR tends to produce a denser point cloud than photogrammetry, however due to the mobile nature of data collections, the LiDAR point clouds are not as dense. After numerous conversations with Michael Butler from UDOT on this topic, LiDAR point cloud sparsity may be due to the nature of the data collections. Mandli most likely uses certain technologies to help conduct data collections to ensure sufficient data is collected without gathering unnecessary data. For example, the sensors must be gathering data at a much faster rate while on a highway than when the vehicle is exiting or coming to a stop. If the sensors continued to gather data while the vehicle is stopped at the same speed it gathers data on the highway, there would simply be too much unnecessary information gathered. Therefore, Mandli most likely uses technology that allows them to control collected data. The GoPro Hero 8+ used in this case study does not have the ability to limit the amount of data gathered. It captures as much data as possible from each frame, and with the right conditions, these frames create very dense models.

Another factor that affected the quality and data evaluations was the number of frames per second used to extract frames from videos. Numerous different frames per second were tested such as 100 FPS, 90 FPS, 50 FPS, etc. It was found that having 100 frames was a bit unnecessary, and most good models were created using 50 FPS. Fifty FPS was used for most of the models due to the fact that this was usually a good number of frames for each model without having too many frames making the file size larger than it needs to be. Data processing was also affected by the number of frames per second used. Using a large number of images (such as 100 FPS) can cause data processing times upwards of nine to ten hours. However, whenever 50 FPS was used, data processing times were cut in half with an average processing time of around four to six hours.

Table 4 – Data collection and processing for asset management models

Model	Lighting Conditions	Acquisition Time	Traveling Speed (MPH)	Model Length (Miles)	Number of Registered Images (Aligned/Total)	Processing Time (Image-Based)	Number of Points
Model 1	Dense clouds, intermittent light	18 sec	50	0.25	999/999	2 hr 11 min	410 Million
Model 2	Sunny, perfect sign visibility, no reflections	20 sec	45	0.25	1195/1195	2 hr 48 min	430 Million
Model 3	Sunny, perfect sign visibility, no reflections	18 sec	20 (Exit)	0.1	1026/1026	2 hr 58 min	771 Million
Model 4	Bright sunlight, many reflections	40 sec	45	0.5	850/850	2 hr 5 min	776 Million
Model 5	Indirect sunlight, low light on signs	20 sec	45	0.25	850/850	2 hr 41 min	706 Million
Model 6	Sunny, good sign visibility	18 sec	40	0.2	1107/1301	3 hr 42 min	1.3 Billion

Table 5 – Data Processing Table

Date & Time	Road Location	Miles Driven During Collection Procedures	Model Length (Miles)	Driving Direction (N,S,E,W)	Recording Settings	Speed Limit (MPH)	Actual Speed (MPH)	Road Condition/Material	Camera Position	Angles (0° is straight forward)	Number of frames used per second (FPS)	Total number of images input vs. total number of registered images	Point cloud generation time	Number of Points	Median Key points per image	Median tie points per image	Reprojection Error (RMS)
1/14/2020, 12:45 PM	1300 S Between 900E and Lincoln Street	12	0.5	Driving East	2.7K @ 30 FPS	30	25	Asphalt, lots of black streaks from assumed crack repairs	Centered on hood	0°	30	-	-	55 million (1 point cloud)	-	-	-
2/08/2020, 1:45 PM	Driving North on 900W between 1700S and 1300S	5	0.25	Driving North	2.7K @ 30 FPS	30	25	The road appeared to be asphalt but had sections of road repairs	Centered on hood	0°	30	-	-	90 Million	-	-	-
2/11/2020, 2:00 PM	1300 S between 700E and 1100E	8	0.75	Driving East	4K @ 30 FPS, Linear	30	30	Asphalt, lots of black streaks from assumed crack repairs	Centered on hood	0°	30	-	-	60 million per cloud	-	-	-
2/14/2020 1:00PM	I-15N	18	0.5	Driving North	2.7k @ 120 FPS, Linear	70	60	typical highway	Centered on hood	0°	20	262 Total, 262 Registered	4 hr 36 min	65 million	6,401	361	0.56 pixels
2/17/2020, 2:00 PM	1300 S between 700E and 1100E	8	0.25	Driving East	4K @ 30 FPS, Linear	30	30	Asphalt, lots of black streaks from assumed crack repairs	Centered on hood, but the camera angle was pointed downwards to focus on the roadway	0°	-	-	-	1 billion	-	-	-
2/19/2020, 2:00PM	I-15N	25	0.5	Driving North	2.7K @ 120 FPS, Wide	65	60	typical highway	Centered on hood	0°	70	1302 Total, 1302 Registered	9hr 44min	100 million - 200 million per cloud	5,578	1,001	0.49 Pixels
2/19/2020, 2:00PM	I-215N	23	0	Driving North	1080P @ 120 FPS, Linear	65	60	typical highway	Centered on hood	0°	25	272 Total, 266 Registered	17 min 42 sec	57 million	3,131	21	0.55 pixels
2/20/2020, 11:00 AM	I-215N	17	0.5	Driving North	2.7k @ 60 FPS, Linear	65	~60	typical highway	Centered on hood	0°	30	420 Total, 420 Registered	1 hr 3 min	230 million	5,365	280	0.6 pixels
2/20/2020, 12:00 AM	I-15N	19	0.5	Driving North	4k @ 60 FPS, Wide	65	60	typical highway	Centered on hood	0°	-	-	-	900 million	-	-	-

Table 5 cont. – Data Processing Table

2/21/2020, 2:00 PM	I-201 East	15	1	Driving East	2.7K @ 60 FPS, Linear	65	60-65	rough highway with ongoing construction	one view left, one center, one right	-15°,0°,15°	40	803 Total, 788 Registered	2 hr 43 min	110 million	5,960	186	0.64 pixels
2/23/2020, 3:00 PM	I-15N	25	0.5	Driving North	4K @ 30 FPS, Linear	65	55	typical highway	one view left, one center, one right	-10°,0°,10°	30	Could not get photos aligned	-	-	-	-	-
3/15/2020, 9:45 AM	I-15N	14	0.5	Driving North	1 run with 4K @ 60 FPS and 2 runs with 2.7K @ 120 FPS	65	45-55	typical highway	Centered on hood	0°	92	1195 Total , 1195 Registered	5 hr 38 mins	430 Million Points (5 Tiles)	5,504	729	0.45 pixels
3/15/2020, 11 AM	I-15N	12	0.5	Driving North	2.7k @ 120 FPS, Wide	65	55-60	typical highway	Centered on hood	0°	53	952 Total, 952 Registered	4 hr 20 mins	805 Million Points (3 tiles)	5,413	348	0.52 pixels
3/23/3030, 10:45 AM	I-15N	10	0.5	Driving North	2.7K @ 120 FPS, Wide	65	55	typical highway	Centered on hood	0°	60	1057 Total, 1057 Registered	NA	NA	5,489	490	0.51 pixels
3/23/2020, 10:45 AM	Continuation of above with less images	-	-	-	-	-	-	-	-	-	50	999 Total, 999 Registered	4 hr 19 min	410 Million points	5,485	436	0.55 pixels
3/24/2020, 11:00 AM	I-15N Exit	6	0.2	Exit north then turn south	2.7K @ 120 FPS, Wide	25	20	typical highway	Centered on hood	0°	43	1026 Total, 1026 Registered	6hr 58 min	771 Million	5,467	837	0.43 pixels
4/28/2019 5:30 PM	Driving East on I-80 just before merging with I-15	23	0.3	Driving East	2.7K @ 120 FPS, Wide	65	50	typical highway	Centered on hood	0°	50	850 Total, 850 Registered	4hr 5 min	776 million	5,421	844	0.48 pixels
4/28/2020 5:30 PM	Driving East on I-80 while merging with I-15	23 (same trip as above)	0.5	Driving East	2.7k @ 120 FPS, Wide	65	45	typical highway	Centered on hood	0°	50	850 Total, 850 Registered	5hr 41 min	706 million	14,910	1,165	0.61 pixels

Table 5 cont. – Data Processing Table

5/6/2020 6:00PM	I-15N	0 miles driven. Reprocessing old video	0.5	Driving North	2.7k @ 120 FPS, Wide	60	45-55	typical highway	Centered on hood	0°	50	728 Total, 728 Registered	1hr 42 mins	200 Million	14,473	815	0.6 pixels
5/9/2020 5:00PM	I-15N	34	0.25	Driving North	4K @ 60 FPS, Wide	60	45-50	typical highway	Centered on hood	0°	50	729 Total, 729 Registered	11 hrs 9 min	1.7 Billion points	6,451	136	0.46 pixels
5/11/2020 5:00 PM	I-15N	34 (same trip as above)	0.25	Driving North	4k @ 60 FPS, Linear	60	45-50	typical highway	Centered on hood	0°	50	761 Total, 761 Registered	9hr 37 min	1.7 Billion points	31,080	398	0.63 pixels
5/17/2020, 3:00 PM	I-15S	44	1	Driving South	2.7k @ 120 FPS, Wide	65	50-55	typical highway	Centered on hood	0°	50 and 60	Could not get photos aligned	-	-	-	-	-
5/17/2020, 3:30 PM	I-15N	44 (same trip as above)	0.25	Driving North	2.7k @ 120 FPS, Wide	65	40-45	typical highway	Centered on hood	0°	50 and 90	Could not get photos aligned	-	-	-	-	-
5/17/2020, 4:00 PM	I-80E	45 (same trip as above)	0.25	Driving East	2.7k @ 120 FPS, Wide	65	45-50	typical highway	Centered on hood	0°	50	802 Total, 802 Registered	2 hr 20 min	150 million points	5,295	828	0.49 pixels
5/17/2020, 4:00 PM	I-80E	46 (same trip as above)	0.25	Driving East	2.7k @ 120 FPS, Wide	65	55-60	typical highway	Centered on hood	0°	50	Could not get photos aligned	-	-	-	-	-
5/18/2020, 4:00 PM	I-15S Exit 305 C-A	23	0.25	Driving South	2.7k @ 120 FPS, Wide	65	40-50	typical highway	Centered on hood	0°	50	1301 Total, 1107 Registered	9 hr 42 minutes	1.3 Billion (Downsample d to 500 Million to make easier to work with)	13,171	1,209	0.59 pixels
6/2/2020, 1:00 PM	Driving North on 700W between 2100S and 1700S	8	<0.1	Driving North	2.7k @ 120 FPS, Wide	25	40 MPH	City street with lots of streaks and repairs	Centered on hood	0°	120	648 Total, 648 Registered	6hr 38 min	350 million (300 million cleaned)	18,450	2,776	0.43 pixels
43985	North	9	0.1	Driving North	2.7k @ 120 FPS, Wide	26	30 MPH	City street with lots of streaks and repairs	Centered on hood	0°	90	596 Total, 596 Registered	4hr 56 min	267 million (217 cleaned)	17,524	2,830	0.44 pixels

4.2.1 Accuracy Assessment and Quality Assessment

Table 6 below shows a comprehensive overview of all sign ratios (height to width) extracted from both image-based and LiDAR-based point clouds. Signs were separated into small, medium, and large sign groups, and an overall error encompassing all signs was also calculated. From our findings, the image-based point cloud's overall relative error was within 1% of the relative errors of the LiDAR-generated point clouds. It is worth noting that some signs from both image-based and LiDAR-based point clouds were excluded as outliers due to the fact that there were not enough generated points of that particular sign in order to get an accurate sign ratio measurement. Poorly generated signs can be due to a number of factors such as distance from sensor, vehicular obstructions, and environmental conditions causing too much reflection on the sign. These outliers were not native to image-based point clouds, as there were some signs in the LiDAR-generated point clouds that were also too poor to extract an accurate measurement from. In the following sections, each point cloud model will have a more in-depth individual description that will give an overall summary of the generated point cloud and its comparison to the corresponding LiDAR point cloud. There is also a standard deviation and coefficient of variation (CV) for each point cloud. These values are meant to provide an overall description of the point cloud's density distribution. A higher coefficient of variation means that the point cloud is less uniform. As can be seen in Table 6, the LiDAR point clouds have a lower CV value, meaning they are slightly more uniform than the image-based point clouds. Another thing to note is the visibility of the signs depending on the size of the sign. For the most part in the photogrammetry models, large signs such as overhead signs are easy to read and usually generated in a good fashion. As the signs get smaller they tend to become less legible, however they still have good geometric data and sign ratios can be extracted from them. Signs such as mile marker signs, and some other signs such as speed limit signs can be slightly hard to read. However, spatial data is conserved and sign ratios can still be measured.

Table 6 – Measurement overview from image-based and LiDAR-based point clouds for asset management

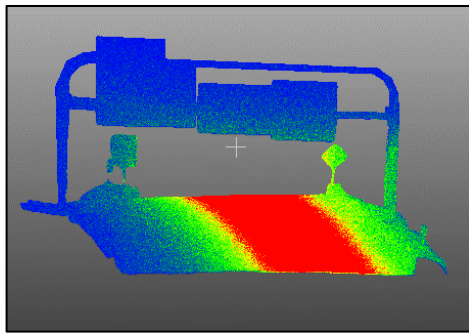
Model	Sensing Technology	Sign Ratio Errors (%)			Overall Model Error (%)	Average Sign Density (Points/in ²)	Standard Deviation of Sign Density	Coefficient of Variation of Sign Density (CV)
		Small	Medium	Large				
Model 1	Image-Based	2.11	6.89	4.70	5.09	35.3	18.4	0.52
	LiDAR	4.39	5.40	1.51	3.93	0.74	0.32	0.44
Model 2	Image-Based	1.68	7.40	6.42	5.35	14.7	5.38	0.37
	LiDAR	2.78	1.56	6.41	3.81	0.89	0.37	0.42
Model 3	Image-Based	5.90	4.69	6.96	5.16	35.4	13.1	0.37
	LiDAR	2.96	2.91	4.25	3.48	0.96	0.41	0.42
Model 4	Image-Based	3.61	2.56	5.92	3.94	21.9	12.2	0.56
	LiDAR	1.71	2.15	4.93	2.81	0.61	0.20	0.33
Model 5	Image-Based	3.61	2.56	5.92	3.51	38.8	24.8	0.64
	LiDAR	1.71	2.15	4.93	2.73	0.91	0.47	0.52
Model 6	Image-Based	1.22	4.45	3.29	2.92	28.0	13.7	0.49
	LiDAR	1.23	3.27	3.47	4.11	1.63	0.67	0.41
Averages	Image-Based				4.33	29.0	14.6	0.49
	LiDAR				3.48	0.96	0.41	0.42

4.2.2 Model 1

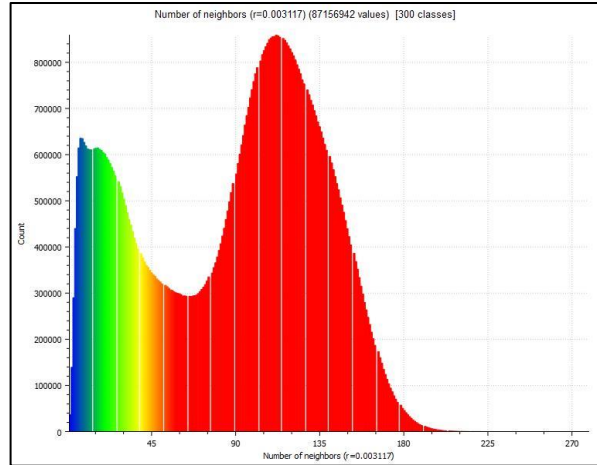
Model one was one of the first highway models generated. A large LiDAR roadway point cloud section was obtained from UDOT, and then it was split into three sections to make data processing a bit smoother. Model one was the first portion of the LiDAR point cloud obtained. Signs and pavement marking in this particular model were generated nicely, however this stretch of roadway passes under two bridges which caused a slight disruption within the model. The bridges cast a dark shadow on the road, and the lighting changes dramatically while passing under the bridges. This caused a slight break and skew in the model under the first bridge, but for the most part signs were unaffected. There was one mile-marker sign directly under this first bridge in the shadows, and this sign was not generated very well. This mile marker sign was one of the aforementioned outliers, and as you can see in Table 7, the relative error for this particular sign was almost 50 percent. Other than the singular mile marker sign, all other signs for this model were generated nicely and most relative errors are considerably low. Also, below the table you will see information regarding the density of this model compared to the density of Mandli's model. As mentioned before, the density of generated points in the photogrammetry model is denser than the density of generated points for the LiDAR model. One thing you will notice in this model and in others is the saturation of generated points in the model. Both image-based and LiDAR-based models have a higher saturation closer to the data acquisition sensor. As generated points get farther from the sensor, they become less dense and slightly more distorted.

Table 7 – Model 1 Sign Ratio Table

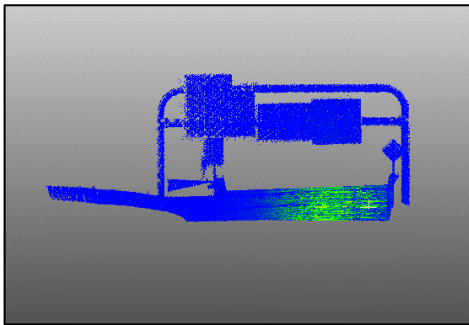
Sign Size	Image-Based Measurements									LiDAR-Based Measurements						
	Image from model	Height	Width	Ratio (H/W)	Sign Density (Points/in ²)	Image of actual sign	Sign Code (MUTCD)	Actual Ratio (H/W)	Percent Error	Image	Height	Width	Ratio (H/W)	Sign Density (Points/in ²)	Actual Ratio (H/W)	Percent Error
Small		0.3	0.1	3	37.28		D10-A	3	1.48E-14		0.96	0.34	2.82	0.69	3.00	5.88
Small		Sign not fully generated	Sign not fully generated	Sign not fully generated	Sign not fully generated		Sign not fully generated	Sign not fully generated	Sign not fully generated		0.93	0.31	3.00	0.97	3.00	0.00
Small		0.25	0.087	2.87	31.37		D10-A	3	4.21		0.89	0.32	2.78	0.40	3.00	7.29
Medium		0.5	0.38	1.32	56.02		R2-1	1.25	5.26		1.51	1.19	1.27	0.68	1.25	1.51
Medium		0.53	0.4	1.33	30.89		E5-1C	1.5	11.67		2.06	1.44	1.43	0.47	1.50	4.63
Medium		0.41	0.41	1.00	73.16		W4-2R	1	0.00		1.65	1.53	1.08	0.96	1.00	7.84
Medium		0.45	1.13	0.40	13.28		E1-5BP	0.36	10.62		1.41	3.64	0.39	0.34	0.36	7.60
Large		1.08	1.7	0.64	22.68	Sign Varies	E6-2A	0.68	6.09		3.62	5.48	0.66	0.50	0.68	2.35
Large		0.86	1.26	0.68	28.47	Sign Varies	E6-2A	0.6667	2.38		2.92	4.35	0.67	1.02	0.67	0.69
Large		1.03	1.06	0.97	24.55	Sign Varies	E6-2A	0.92	5.62		3.52	3.77	0.93	1.33	0.92	1.49



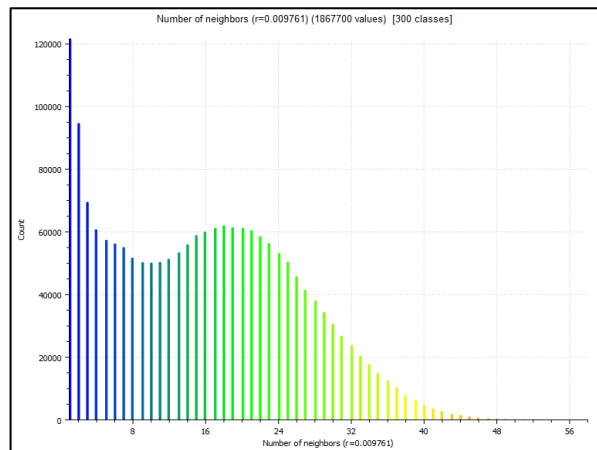
(a)



(b)



(c)



(d)

Figure 10 – Comparison of point cloud density for model 1. Number of Neighbors Density for (a) image-based model section saturation, (b) image-based model histogram, (c) LiDAR model section saturation, (d) LiDAR model histogram

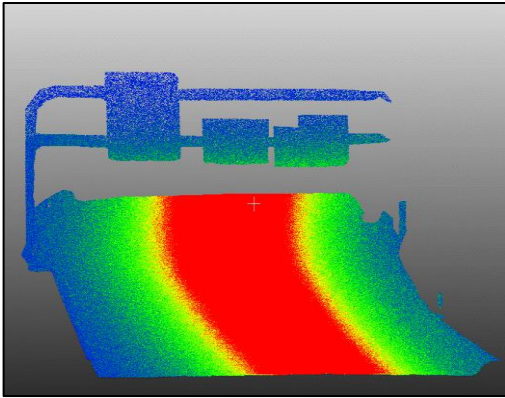
4.2.3 Model 2

Model two is similar to Model one in terms of relative errors and point cloud density. The generated signs in this model are generated well, and this particular model is very dense. This is likely due to the fact that data for this collection was collected on a sunny day and there was limited traffic on this section during this particular time. There was only one sign in this model that was generated poorly. You will notice that some signs in the following tables do not have

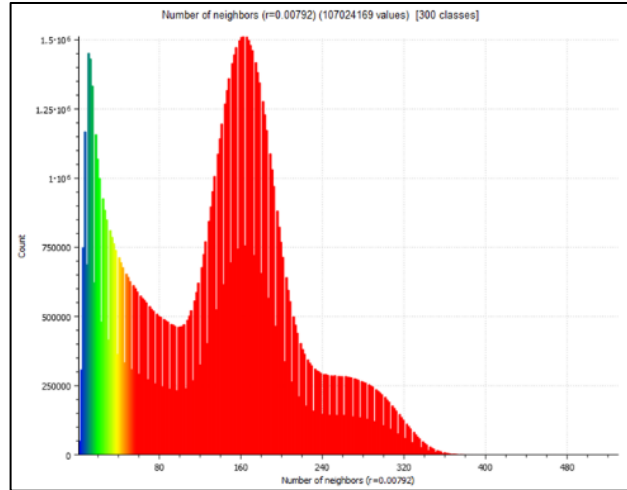
an actual sign ratio. The Utah Standard Highway Sign Supplement, The Manual on Uniform Traffic Control Devices (MUTCD), and UDOT's publicly shared highway sign map overlay was used to find out the actual dimensions of various signs throughout the highways. While these resources were able to provide most of the dimensions, there were a few signs that did not have standard sizes due to varying road conditions. The sign codes are also provided by the Manual on Uniform Traffic Control Devices and UDOT's highway sign map to help the reader have a definite understanding of the exact sign.

Table 8 – Model 2 Sign Ratio Table

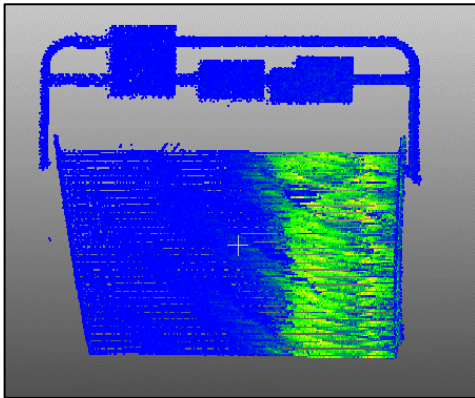
Image-Base Sign Ratios for Model 2											LiDAR-Based Sign Ratios for Model 2								
	Image from model	Location in point cloud (0=beginning, 100=end)	Height	Width	Ratio (H/W)	Sign Density	Image of actual sign	Sign Code	Actual Ratio (H/W)	Percent Error		Image from model	Location in point cloud (0=beginning, 100=end)	Height	Width	Ratio (H/W)	Sign Density	Actual Ratio (H/W)	Percent Error
Small		10	0.67	0.22	3.04545	9.292		D10-A	3	1.5152	Small		10	1.4	0.48	2.91667	0.4259	3	2.77778
		60	0.55	0.18	3.05556	16.28		D10-A	3	1.8519			60	Sign not fully generated	Sign not fully generated	Sign not fully generated	1.3889	Sign not fully generated	Sign not fully generated
Medium		50	1.1	0.95	1.15789	22.76		R2-1	1.25	7.3684	Medium		50	1.58	1.29	1.22481	0.6212	1.25	2.0155
		8	0.88	4.15	0.21205	6.682		E1-5P	0.1974	7.4378			8	0.7	3.5	0.2	0.4956	0.19737	1.33333
		90	Sign not fully generated	Sign not fully generated	Sign not fully generated	-		Sign not fully generated	Sign not fully generated	Sign not fully generated			90	0.7	3.5	0.2	0.8996	0.19737	1.33333
Large		8	5.93	4.88	1.21516	-		E6-2A	Could not find	-	Large		8	5.49	4.48	1.22545	-	Could not find	-
		8	2.97	4.77	0.62264	14.3		E6-2	0.6897	9.717			8	2.7	4.22	0.63981	1.1734	0.68966	7.22749
		8	3.23	7.36	0.43886	18.19		GS2-2	0.4762	7.8397			8	3.23	7.36	0.43886	0.7931	0.47619	7.83967
		90	3.02	2.86	1.05594	-		MS1-9D	Could not find	-			90	5.35	4.45	1.20225	-	Could not find	-
		90	1.53	2.56	0.59766	-		1Yellow	Could not find	-			90	2.71	4.33	0.62587	-	Could not find	-
		90	1.31	2.92	0.44863	15.47		GS3-1	0.4412	1.6895			90	2.3	5.44	0.42279	1.3279	0.44118	4.16667



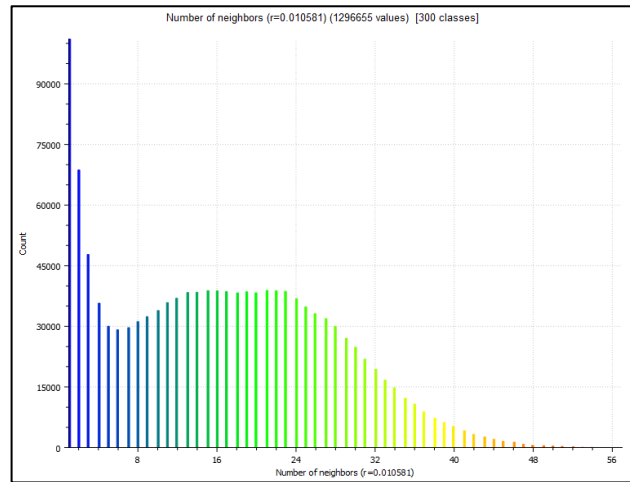
(a)



(b)



(c)



(d)



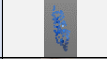











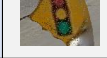






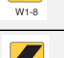

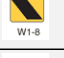

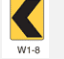
Figure 11 – Comparison of point cloud density for model 2. Number of Neighbors Density for (a) image-based model section saturation, (b) image-based model histogram, (c) LiDAR model section saturation, (d) LiDAR model histogram

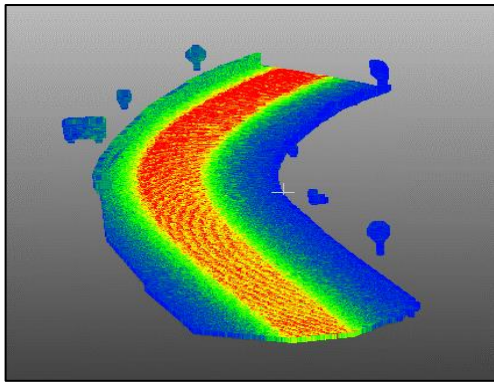
4.2.4 Model 3

Section 3 is the final section of the first large point cloud obtained from Mandli. It is worth noting that this is the densest section of all three sections, and this is due to the fact that section three is an exit roundabout off of the highway. Due to this section being a roundabout

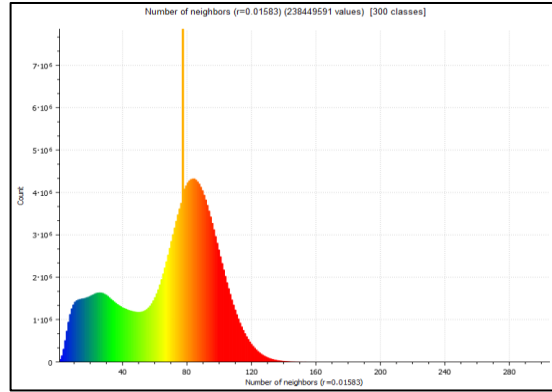
exit, traveling speeds were much slower on this section as opposed to highway traveling speeds for sections one and two. This holds true for the LiDAR model as well. As you can see, the LiDAR model for this particular section is denser than other LiDAR models, which is also due to the speed of data collection. The slower you travel during data collection, the more data the sensor can gather, making point clouds denser the slower you drive. Signs for this section were generated well, however most signs on this roundabout exit were smaller signs on the side of the roadway, and smaller signs tend to be more difficult to generate because of the limited data gathered during data acquisition. Nonetheless, the overall error for this section is less than six percent, and it is still comparable to the LiDAR point cloud.

Table 9 – Model 3 Sign Ratio Table

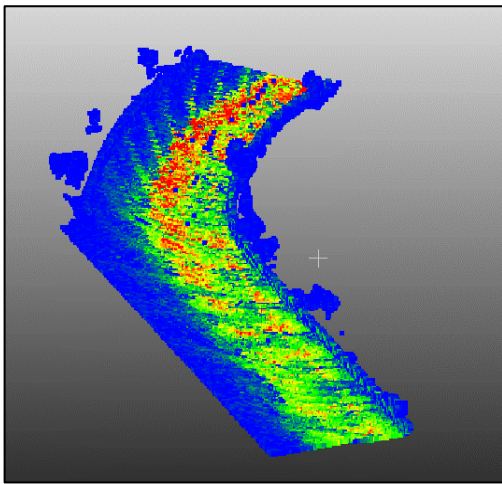
Image-Based Sign Ratio for Model 3											LiDAR-Based Sign Ratio for Model 3								
	Image from model	Location in point cloud (0=beginning, 100=end)	Height	Width	Ratio (H/W)	Sign Density	Image of actual sign	Sign Code	Actual Ratio (H/W)	Percent Error		Location in point cloud (0=beginning, 100=end)	Height	Width	Ratio (H/W)	Sign Density	Sign Code	Actual Ratio (H/W)	Percent Error
Small		5.00	1.48	0.49	3.02	23.40		D10-1A	3.00	0.68	Small	5.00	0.98	0.31	3.16	2.75	D10-1A	3.00	5.38
		15.00	1.30	0.39	3.33	22.82		D10-1A	3.00	11.11		15.00	1.01	0.35	2.89	2.57	D10-1A	3.00	3.81
		85.00	Not Generated	Not Generated	Not Generated			D10-1A	Not Generated	Not Generated		85.00	0.99	0.32	3.09	1.81	D10-1A	3.00	3.13
Medium		10.00	2.40	2.29	1.05	22.38		W1-11	1.00	4.80	Medium	10.00	1.68	1.67	1.01	1.12	W1-11	1.00	0.60
		20.00	1.60	1.14	1.40	34.28		W1-8	1.33	5.26		20.00	0.75	0.59	1.27	0.22	W1-8	1.33	4.66
		25.00	1.96	1.93	1.02	52.30		W3-3	1.00	1.55		25.00	1.10	1.11	0.99	0.38	W3-3	1.00	0.90
		25.00	Not Generated	Not Generated	Not Generated			W3-3	Not Generated	Not Generated		25.00	1.23	1.19	1.03	1.69	W3-3	1.00	3.36
		30.00	1.20	0.99	1.21	37.60		W1-8	1.33	9.09		30.00	0.72	0.53	1.36	0.23	W1-8	1.33	1.89
		50.00	1.13	0.88	1.28	36.17		W1-8	1.33	3.69		50.00	0.83	0.60	1.38	0.21	W1-8	1.33	3.75
		60.00	0.98	0.73	1.34	31.26		W1-8	1.33	0.68		60.00	0.83	0.68	1.22	0.25	W1-8	1.33	8.46
		70.00	0.91	0.74	1.23	30.67		W1-8	1.33	7.77		70.00	0.82	0.59	1.39	0.22	W1-8	1.33	4.24
		80.00	0.82	1.52	0.54			R3-8A	Sign Varies	-		80.00	0.67	1.13	0.59	-	R3-8A	Sign Varies	-
Large		15.00	2.45	4.81	0.51	62.82		ES5-1A13	0.48	6.96	Large	15.00	1.43	2.74	0.52	0.51	ES5-1A13	0.48	9.60



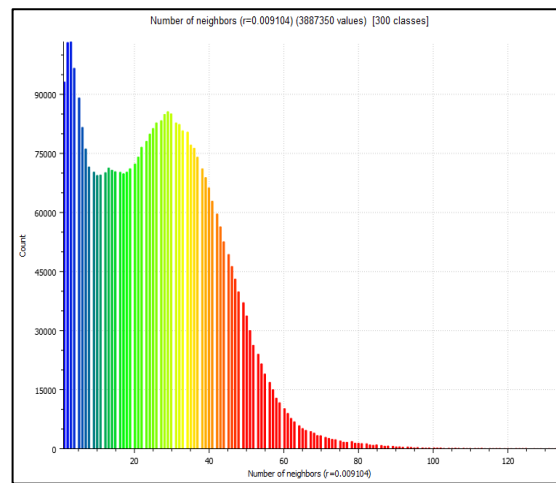
(a)



(b)



(c)



(d)

Figure 12 – Comparison of point cloud density for model 3. Number of Neighbors Density for (a) image-based model section saturation, (b) image-based model histogram, (c) LiDAR model section saturation, (d) LiDAR model histogram

4.2.5 Model 4

This particular section of roadway was from another large LiDAR point cloud. Again, the point cloud was split into separate sections for processing purposes, section 4.2.5 and 4.2.6 are both from this large LiDAR point cloud. Generated signs in this point cloud were generated in a good and acceptable fashion. There are very few problems with this model, however there is one thing worth mentioning. On the right side of the highway on this portion of roadway there is a large wall that runs parallel to the roadway, which causes a large shadow to be cast on portions

of the right side of the road. Fortunately, this shadow did not affect any of the highway signs, but there are some small sections of roadway that are omitted due to the shadow. Data collection for this portion of highway was done closer to normal highway speeds, however the density of the generated model is still very high and much more than the density generated in the LiDAR point cloud.

Table 10 – Model 4 Sign Ratio Table


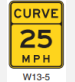





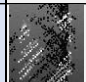




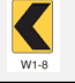
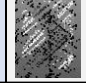
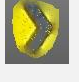

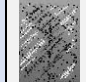
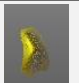

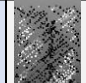
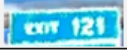
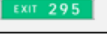



















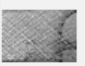






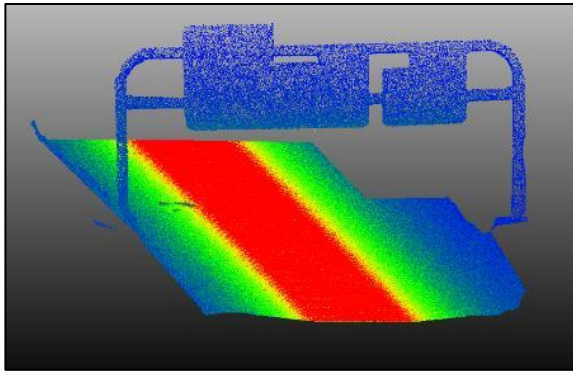
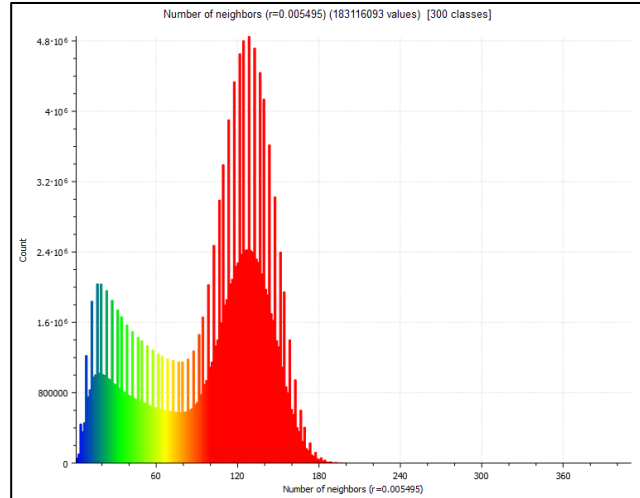
Image-Based Sign Ratios for Model 4											LiDAR-Based Sign Ratios for Model 4								
	Image	Location in point cloud (0=beginning, 100=end)	Height	Width	Ratio (H/W)	Sign Density	Image of Sign	Sign Code	Actual Ratio (H/W)	Percent Error		Image	Location in point cloud (0=beginning, 100=end)	Height	Width	Ratio (H/W)	Sign Density	Actual Ratio (H/W)	Percent Error
Small		25	0.53	0.39	1.359	30.513		W13-5	1.333	1.9231	Small		25	1.087	0.8	1.359	0.664	1.3333	1.906
		25	0.54	0.4	1.35	31.141		W13-5	1.333	1.25		Sign Missing	25	-	-	-	-	-	-
		85	0.55	0.4	1.375	40.192		W1-8	1.333	3.125			85	1.219	0.893	1.365	0.689	1.3333	2.38
		90	0.3	0.65	0.4615	37.45		W1-6	0.5	7.6923			90	0.728	1.481	0.492	0.467	0.5	1.688
		95	0.55	0.43	1.2791	34.899		W1-8	1.333	4.0698			95	1.148	0.86	1.335	0.453	1.3333	0.116
		98	Not Generated	-	-	-		W1-8	-	-			98	1.175	0.867	1.355	0.455	1.3333	1.644
		100	Not Generated	-	-	-		W1-8	-	-			100	1.173	0.858	1.367	0.465	1.3333	2.535

Table 10 cont. – Model 4 Sign Ratio Table

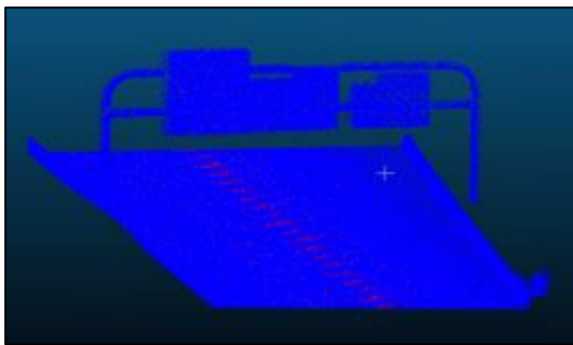
Medium		5	0.35	1.2	0.2917	6.7225		E5-1P	0.278	5	Medium		5	0.719	2.638	0.273	0.61	0.2778	1.88
		5	0.37	1.37	0.2701	7.9531		E5-1P	0.278	2.7737			5	0.781	2.976	0.262	0.358	0.2778	5.524
		20	0.66	1.07	0.6168	24.427		E5-1A	0.625	1.3084			20	1.55	2.41	0.643	0.393	0.625	2.905
		60	0.68	0.67	1.0149	26.691		W1-2A	1	1.4925			60	1.5	1.51	0.993	0.562	1	0.662
		60	0.66	0.67	0.9851	37.489		W1-2A	1	1.4925			60	1.576	1.568	1.005	0.41	1	0.51
		85	0.33	1.15	0.287	7.0991		E5-1P	0.278	3.3043			85	0.723	2.64	0.274	0.798	0.2778	1.409
Large		5	2.57	2.15	1.1953	14.74	Sign Varies depending on needs	GS1-1	1.091	9.5736	Large		5	5.686	4.834	1.176	0.9	1.0909	7.823
		5	1.6	2.35	0.6809	11.176	Sign Varies depending on needs	GS2-1B	0.634	7.365			5	3.498	5.347	0.654	0.74	0.6341	3.162
		5	1.43	2.11	0.6777	13.064	Sign Varies depending on needs	GS6-1A	0.701	3.3408			5	3.13	4.558	0.687	0.483	0.7011	2.06
		85	2.42	2.1	1.1524	11.182	Sign Varies depending on needs	GS1-1	1.091	5.6349			85	5.67	4.84	1.171	0.997	1.0909	7.386
		85	1.46	2.22	0.6577	15.316	Sign Varies depending on needs	GS2-1B	0.634	3.7076			85	3.53	5.34	0.661	0.89	0.6341	4.242



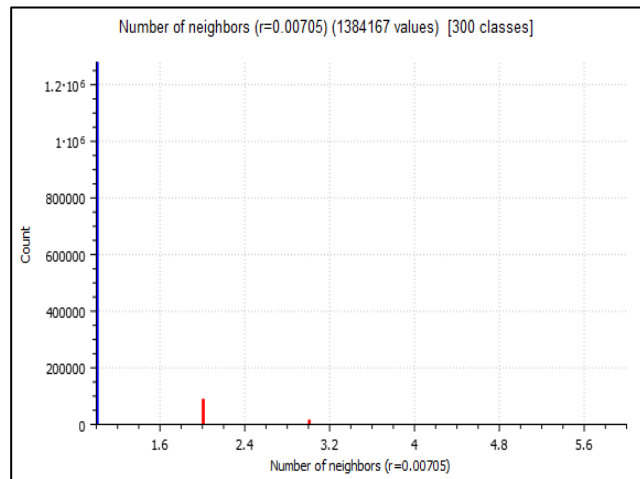
(a)



(b)



(c)



(d)





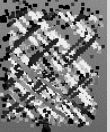

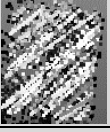





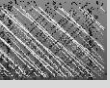




Figure 13 – Comparison of point cloud density for model 4. Number of Neighbors Density for (a) image-based model section saturation, (b) image-based model histogram, (c) LiDAR model section saturation, (d) LiDAR model histogram

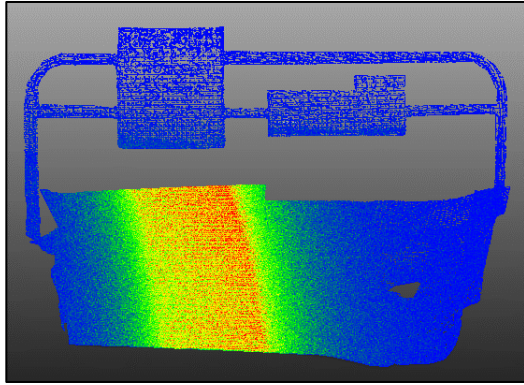
4.2.6 Model 5

This model was the second portion of the previous model mentioned, and the output for this model is also good data. There were not as many signs on this portion of the road, however all of the signs that were on the roadway were generated in an acceptable fashion and sign ratios are also acceptable. This model has a good density, but it is not as dense as the previous portion

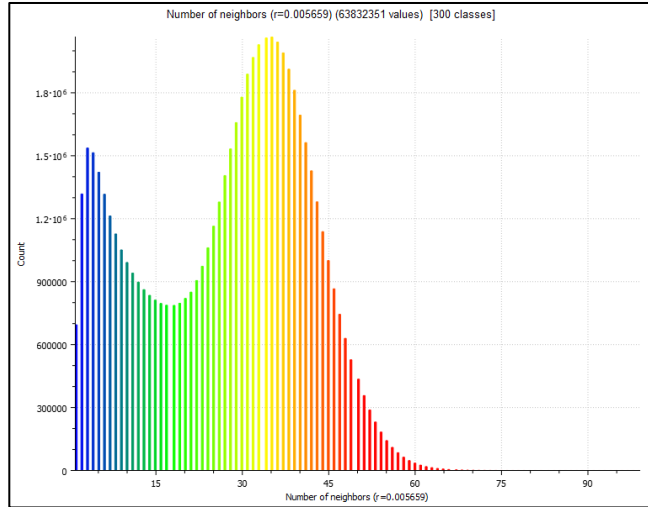
of this roadway. This is most likely caused by the angle of the sun. In section 4.2.5, the traveling direction was eastbound on interstate I-80 in the later hours of the afternoon so the sun was shining from behind while traveling. After the end of the previous model, the road curves to the right and begins heading south, which made the sun directly to the right, rather than behind. From looking at the table of generated signs in this section, you will see that the signs are a bit darker and not as vibrant and crisp as they are in other models. This is also due to the change in sun angle. Nonetheless, the overall quality of the point cloud, generated density, and sign ratio errors are very acceptable and are comparable to other models even though lighting conditions were less than optimal.

Table 11 – Model 5 Sign Ratio Table

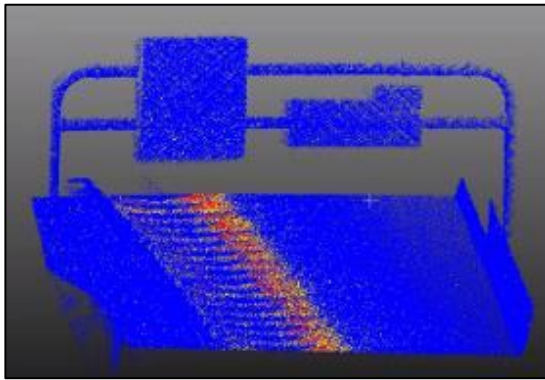
Image-Based Sign Ratio for Model 5											Sign Ratio for Model 5								
	Image	Location in point cloud (0=beginning, 100=end)	Height	Width	Ratio (H/W)	Sign Density	Image of Sign	Sign Code	Actual Ratio	Percent Error		Image	Location in point cloud (0=beginning, 100=end)	Height	Width	Ratio (H/W)	Sign Density	Actual Ratio	Percent Error
Small		30	1.11	0.34	3.26	73.81		D10-5	3.33	2.06	Small		30.00	1.48	0.44	3.34	1.71	3.33	0.16
		70	0.95	0.77	1.23	19.49	Could not find specific sign	Could not find code	1.25	1.30			70.00	1.49	1.17	1.27	0.57	1.25	1.63
		70	0.86	0.69	1.25	58.48	Could not find specific sign	Could not find code	1.25	0.29			70.00	1.41	1.15	1.23	1.05	1.25	1.91
Medium		5	0.67	2.17	0.31	6.88		E5-1P	0.29	4.98	Medium		5.00	0.72	2.34	0.31	0.37	0.29	4.84
		20	1.26	1.94	0.65	58.81		E5-1A	0.63	3.92			20.00	1.46	2.30	0.64	0.73	0.63	1.70
Large		5	5.19	4.5	1.15	26.47	Sign Varies depending on needs	GS1-1	1.09	5.72	Large		5.00	6.15	5.34	1.15	1.31	1.09	5.64
		5	1.95	5.77	0.34	27.39	Sign Varies depending on needs	GS2-1B	0.34	0.87			5.00	2.25	6.70	0.34	0.65	0.34	1.30



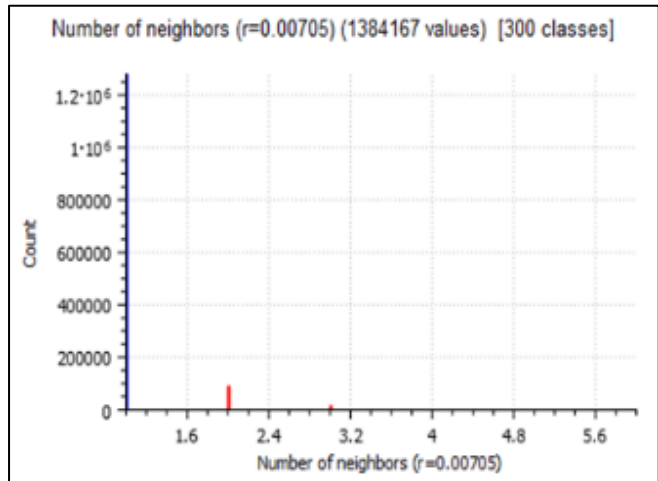
(a)



(b)



(c)



(d)

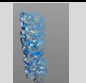

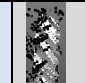


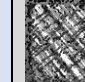




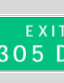
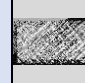


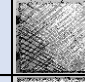



Figure 14 – Comparison of point cloud density for model 5. Number of Neighbors Density for (a) image-based model section saturation, (b) image-based model histogram, (c) LiDAR model section saturation, (d) LiDAR model histogram

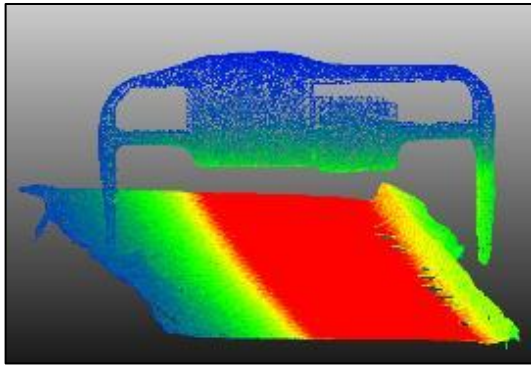
4.2.7 Model 6

This model was also an exit section much like the model in section 4.2.4 of this paper. However, this exit section was linear instead of a roundabout, and traveling speeds were much

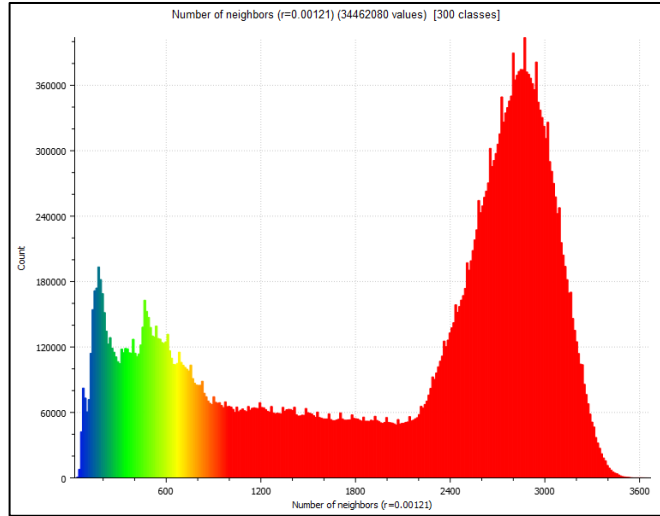
higher because on this exit there were many cars, and there was an option to merge back onto the highway and an option to exit onto 1300S. This higher rate of travel caused a bit of a problem when it came to alignment at first. However, after numerous attempts and trying different settings, an acceptable model was generated with good signs and pavement markings. In Context Capture, image alignment can be done using a few different methods such as: default, exhaustive, and sequential matching. Default uses all images in no particular order and tries to align images to other images that share key points. Exhaustive image alignment uses the same settings as default image alignment, however it does an exhaustive matching algorithm that tries numerous iterations to align images. The best image alignment setting in the asset management case was sequential matching. Sequential matching is best done when images are extracted in a sequential order, such as they are during these linear data collections. With sequential matching, you can set the maximum distance of images. For example, if you set the max image distance to three images, the program will try to align the first image with the next 3 images in the sequence, and once the image is aligned, it will move to the second image and try to match it to the next three images. Different image distances, and also different frames per second for this particular section were tested. Using sequential matching and 50 FPS, a good model with a good overall density and accuracy of generated signs was created.

Table 12 – Model 6 Sign Ratio Table

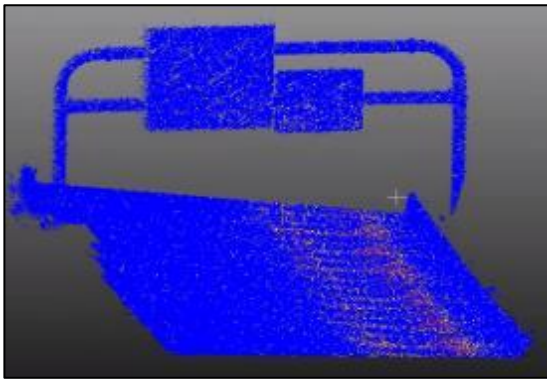
Image-Based Sign Ratio for Model 6											LiDAR-Based Sign Ratio for Model 6								
	Image	Location in point cloud (0=beginning, 100=end)	Height	Width	Ratio (H/W)	Sign Density	Image of Sign	Sign Code	Actual Ratio	Percent Error		Image	Location in point cloud (0=beginning, 100=end)	Height	Width	Ratio (H/W)	Sign Density	Actual Ratio	Percent Error
Small		5	0.01	0.00	3.12	33.40		D10-1A	3.00	3.97	Small		5	0.93	0.32	2.89	0.61	3.00	3.65
		70	0.02	0.01	1.30	46.17		W13-2	1.33	2.82			70	1.50	1.16	1.29	2.18	1.33	3.02
Medium		5	0.04	0.03	1.32	19.45		E5-1A	1.36	3.47	Medium		5	2.50	1.72	1.45	1.28	1.36	6.59
		85	0.02	0.04	0.47	30.46		E5-1A	0.48	1.73			85	1.55	3.16	0.49	2.00	0.48	3.01
Large		50	0.07	0.08	0.89	10.31		E1-1A	0.86	2.58	Large		50	5.15	5.71	0.90	2.09	0.86	4.31
		50	0.04	0.05	0.85	-		E6-2A	Could not find ratio	-			50	3.11	3.83	0.81	-	Could not find	-



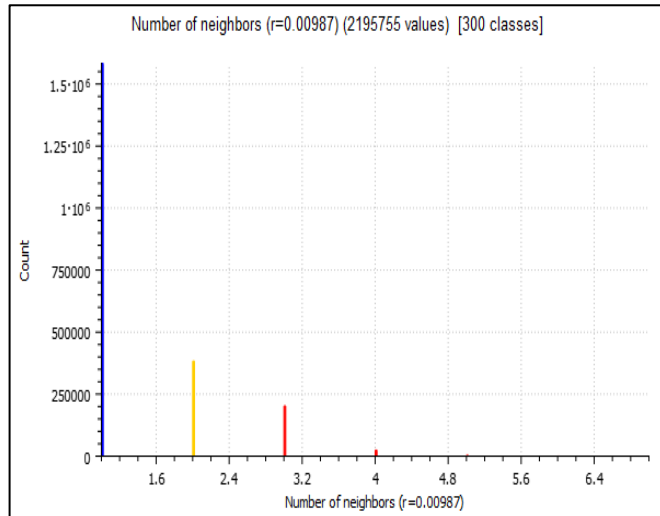
(a)



(b)



(c)



(d)

Figure 15 – Comparison of point cloud density for model 6. Number of Neighbors Density for (a) image-based model section saturation, (b) image-based model histogram, (c) LiDAR model section saturation, (d) LiDAR model histogram

4.3 Unmanned Aerial System Data

The point clouds that were created using aerial data had a slightly different outcome than the point clouds that were created with the mobile GoPro procedures. The length of reconstructed highway is about one quarter of a mile (Figure 16). The UAS LiDAR took about

eight minutes to complete the data collection, while the DJI drone took about six minutes to collect data along the same section. Due to the direction of the LiDAR scanner on the drone, overhead and side signs were unable to be captured within the model. The DJI drone was angled 60 degrees below the horizon, therefore it was able to capture overhead and side highway signs. However, due to the height that the drone was flying at, nearly all of the signs were not generated dense enough to extract measurements. More than 97% of the generated points within the image-based point cloud have no neighbor within a circle of radius 4cm. Though the sign measurements were not generated perfectly, their locations within the model are still accurate enough to extract location information for the purposes of asset mapping. The drones are also able to accurately map terrains as shown in Figure 16. The drone-based data acquisition procedures could also be used for highway bridge inspections, though a more thorough data review would need to be completed. Daj et al. (2013) recommends a distance of less than 25 meters [19]. Popescu et al. (2019) recommends to be as close as 15 meters [20]. Overall, it is up to the engineer to decide which technology above would be most beneficial to their case. More case studies would be necessary for a more in-depth assessment of the capabilities of the drones with respect to the case studies at hand.

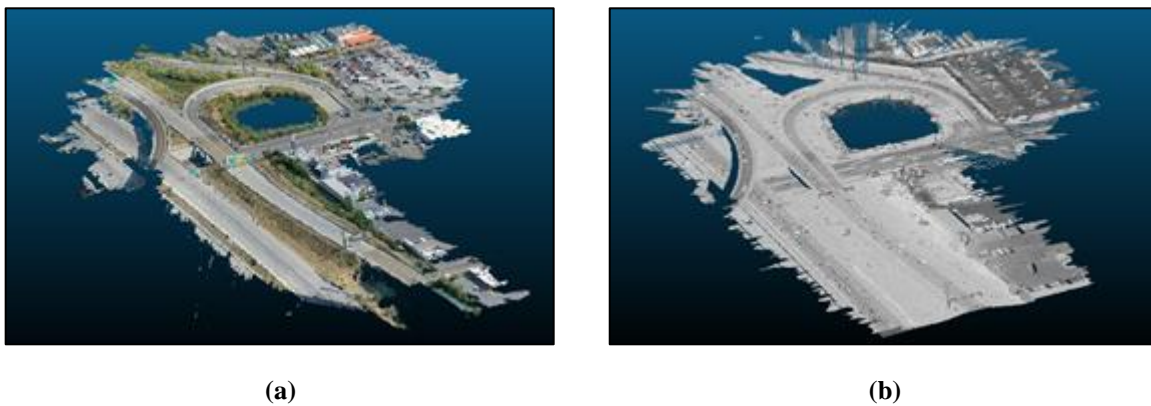


Figure 16 – Comparison between (a) DJI Mavic Pro 2 point cloud using photogrammetry and (b) DJI M600 Drone point cloud with LiDAR

4.4 Pedestrian Access Ramp

Pedestrian access ramp data was evaluated quite differently from asset management data. The most important aspect of pedestrian access ramp data is ensuring that the ramp components

are within specifications and their requirements are met. It was of interest to the researchers to see how accurate extracted point cloud measurements could be, and whether or not they line up with inspections that are done in the field according to UDOT’s specifications. Evaluation of pedestrian access ramps are a bit more straightforward and they include measuring the slope of various areas, and the distances of those areas to ensure that they are passing per UDOT’s standards. In the following sections you will see tables including measurements that were extracted from point clouds (Table 13), and you will also see the UDOT C-170 evaluation form that was used to compare in-field measurements to extracted point cloud measurements.

Table 13 – Pedestrian access ramp slope errors

Pedestrian Access Ramp Model	Technology	Slope Error (%)
Ramp 1	Photogrammetry	0.60
	LiDAR	0.27
Ramp 2	Photogrammetry	0.28
	LiDAR	0.19
Ramp 3	Photogrammetry	0.28
	LiDAR	0.16
Ramp 4	Photogrammetry	0.35
	LiDAR	0.19
Ramp 5	Photogrammetry	0.24
	LiDAR	0.18
Ramp 6	Photogrammetry	0.16
	LiDAR	0.14
Average Error	Photogrammetry	0.32
	LiDAR	0.19
Standard Deviation	Photogrammetry	0.15
	LiDAR	0.04
Coefficient of Variation	Photogrammetry	0.48
	LiDAR	0.24

Table 14 – Data Processing Table for Pedestrian Access Ramps













Ramp	File Name	Image	Location	Inspection	Number of	Number of	Quality of Point Cloud	Processing Settings	Keypoints	Tie Points	RMS
Ramp 1	D:\Research\Pedestrian Access Ramps\Ramp 1			Ramp 1	31 Photos Total, 31 aligned	258,651,814	Point Cloud Quality is great. I think It is due to the large camera sensor size that I was using. Also the lighting was a good sunny day with little to no clouds.	Aerotriangulation took 2 minutes and 40 seconds. I used the default image alignment that context capture offers, the only thing I changed is keypoint density from normal to high. All images were aligned correctly. The point cloud size before processing was 9.8 Gb and no tiles were needed. The point cloud was processed in 44 minutes and 22 seconds. Model processed without a flaw	Median of 47,166 keypoints per image	Median of 384 tie points per photo	0.69 pixels
Ramp 2	D:\Research\Pedestrian Access Ramps\Ramp 2			Ramp 2	37 Photos total, 37 aligned	429,797,343 (295,559,874 Cleaned)	Great point cloud quality	Aerotriangulation took 4 minutes and 10 seconds. I used the default image alignment that context capture offers, the only thing I changed is keypoint density from normal to high. All images were aligned correctly. The point cloud size before processing was 5.9 Gb and no tiles were needed. The point cloud was processed in 48 minutes and 12 seconds. Model processed without a flaw	Median of 46,394 keypoints per image	Median of 162 tie points per image	0.75 pixels
Ramp 3	D:\Research\Pedestrian Access Ramps\Ramp 3			Ramp 3	29 total photos, 27 aligned	313,767,481 (153.790,452 Cleaned)	Great point cloud quality	Aerotriangulation took 4 minutes and 14 seconds. I used the default image alignment that context capture offers, the only thing I changed is keypoint density from normal to high. Only 2 images could not be aligned because they were too close and there was nothing to distinguish it in the photo. The point cloud size before processing was 7.4 Gb and no tiles were needed. The point cloud was processed in 48 minutes and 12 seconds. Model processed without a flaw	Median of 46400 keypoints per image	Median of 189 tie points per photo	0.73 pixels

Table 14 cont. – Data Processing Table for Pedestrian Access Ramps

Ramp 4	D:\Research\Pedestrian Access Ramps\Ramp 4			Ramp 4	31 total photos, 31 aligned	264,338,208	Great point cloud quality	Aerotriangulation took 3 minutes and 10 seconds. I used the default image alignment and only changed keypoint density to high. All images were properly aligned. The point cloud size before processing was 10 GB, no tiling was needed. It took 43 minutes and 58 seconds to process. Model processed without a flaw.	Median of 22776 keypoints per image	Median of 524 tie points per photo	0.64 pixels
Library Ramp	D:\Research\Pedestrian Access Ramps\Library Ramp			No Inspection Report	29 total photos, 27 aligned	436,552,997 (267,786,121 Cleaned)	Point Cloud quality is great. Very clean model	Aerotriangulation took 1 min and 23 seconds. I used the default alignment settings, but changed keypoint density to high and pair selection mode to exhaustive. I also allowed component construction mode to do multiple passes. Only two images were unable to be aligned, even after numerous alignment efforts. The point cloud size before processing was 5.9 GB so no tiling was needed. Processing was interrupted by a computer crash but finished with no problems after the computer rebooted. Processing took about 50 minutes.	Median of 46968 keypoints per image	Median of 125 tie points per photo	0.74 pixels
4th West & 3rd North	D:\Research\Pedestrian Access Ramps\4th West and 3rd North			No Inspection Report	25 total photos, 24 aligned	247,958,617 (162,860,993 Cleaned)	Point cloud quality is good, however it is not the most dense or best point cloud. It should serve this purpose well though.	Aerotriangulation took 1 min and 20s. I used the default aerotriangulation settings. Normal keypoint density, default pair selection mode, and one pass for component construction mode. Aerotriangulation took a few tries and the first few times I was unable to get 8 of the images aligned. I decided to use GCP's in the images that weren't aligned and referenced the same GCP in the images that were aligned. After this I was able to get all but 1 image aligned.	Median of 26,733 keypoints per image	Median of 352 tie points per photo	0.63 pixels

4.4.1 Ramp 1

Ramp 1 is a pedestrian access ramp near University Hospital. As you can see below in Figure 18 (c), comparing the extracted measurements to UDOT's in-field measurements, the error between the measuring procedures was 0.6% for photogrammetry and 0.27% for LiDAR. This error is excluding the one outlier measurement of one of the flares of the pedestrian access ramp. It is believed that the measurement extracted from the point cloud is the more accurate measurement of the two. The flare is only about a foot long, and during the in-field inspections a four-foot-long level was used to measure the slope of this particular component. There was a lot of overhang of the level while measuring this area which leads us to believe that it could lead to a bad slope reading. Even after measuring the slope of that flare separately in the field with a Leica Disto D5, slope readings were around 22%, which corroborates the measurement extracted from the point cloud. Regardless of this one outlier, all other slopes are very close to the extracted slopes from the field.

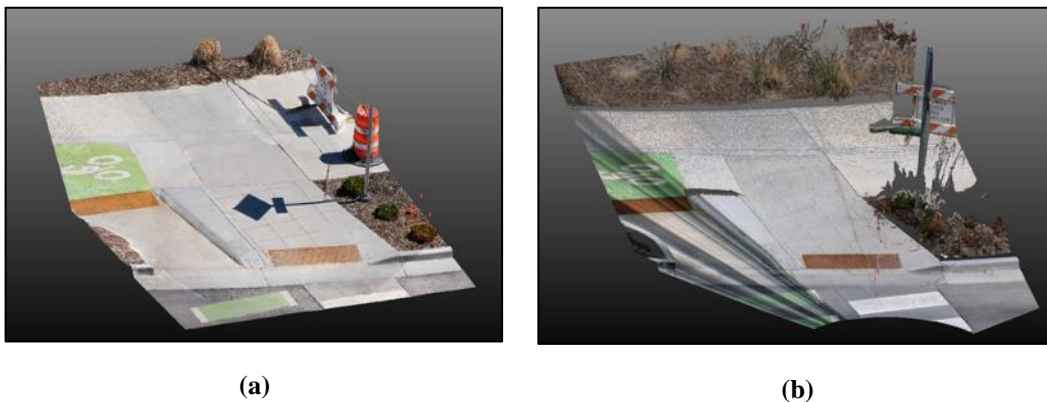


Figure 17 – Ramp 1 point clouds using (a) photogrammetry and (b) LiDAR

UDOT C-130 Pedestrian Access Evaluation Form
 Refer to UDOT 74 Series Standard Drawings for complete requirements
 March, 2020

Project: **15 RD 1100-1** City: **St. George** County: **DC**

Date: **03/10/2020** City: **St. George** County: **DC**

Primary: **5** Sub: **1** Signal: **Stop/Thru** Signal: **Stop/Thru**

Secondary: **1** Signal: **Stop/Thru** Signal: **Stop/Thru**

NOTES:
 1. If a corner or location has multiple accesses, complete a separate form for each.
 2. Inventory accesses from the roadway facing the corner/back of access; provide unique and repeatable identifiers
 3. Construction tolerances - all slopes must be within 0.04% of intention
 4. Document substandard sidewalks without an approved Technical Infeasibility. Accesses will not FAIL due to substandard sidewalks
 5. Waive compliance to adjacent sidewalk cross slopes within at least one panel.
 6. Document substandard crosswalks without an approved Technical Infeasibility. Accesses will not FAIL due to substandard crosswalks
 *Cross Slope Criteria: 0.2% if controlled by Stop/No-Stop; 0.5% if not controlled by Stop/No-Stop (including signals); Max: Road Grade at Midblock

Access Type: Parallel, Perp, Curbside, At-Grade, Directional

Access Location: Multiple Crosswalks, Corner, N, S, E, W, SW, SE, NW, NE

Measurement and Dimensional (Pass/Fail)

Element	Item (Pass Criterion)	Location	Location	Location	Location	Comments
Midblock	Levelled joints on curb breaks	Yes	No	Pass	Fail	
	Width (x 4 ft)	6.7	6.7	Pass	Pass	
Pedestrian Access Route (PAR)	Cross Slope ($\le 2.0\%$)	2.1%	1.1%	Fail	Fail	
	Running Slope ($\le 2.0\%$)	0.9%	0.9%	Pass	Pass	
Flare	Width (4 min)	6.7	6.7	Pass	Pass	
	Running Slope ($\le 2.0\%$)	0.9%	0.9%	Pass	Pass	
Turning Space (T)	Depth (Minimum of min, Corner: 5' max)	6	6	Pass	Pass	
	Grade Breaks (No)	Yes	No	Fail	Fail	
Ramp (R)	Running Slope ($\le 2.0\%$)	0.9%	0.9%	Pass	Pass	
	Grade Breaks (No)	Yes	No	Fail	Fail	
Flare (F)	F1 Slope ($\le 2.0\%$)	0.9%	0.9%	Pass	Pass	
	F2 Slope ($\le 2.0\%$)	0.9%	0.9%	Pass	Pass	
Crosswalk (C)	Running Slope ($\le 2.0\%$)	0.9%	0.9%	Pass	Pass	
	Grade Breaks (No)	Yes	No	Fail	Fail	
At-Grade Access (A)	Running Slope (No change to adjacent)	Yes	No	Fail	Fail	
	Cross Slope ($\le 2.0\%$)	0.9%	0.9%	Pass	Pass	
Thruway Island (TI)	Running Slope ($\le 2.0\%$)	0.9%	0.9%	Pass	Pass	
	Grade Breaks (No)	Yes	No	Fail	Fail	

(a)

Element	Item (Pass Criterion)	Location	Location	Location	Location	Comments	
Detectable Warning Surface (DWS)	Type	Polymer Cast Iron Stamped/ Precast	Polymer Cast Iron Stamped/ Precast	Polymer Cast Iron Stamped/ Precast	Polymer Cast Iron Stamped/ Precast		
	Color Contrasts with Surrounding Surface	Yes	Yes	Yes	Yes		
	Squares Full Curb Cut (2' 4" single, 2' 8" dual)	Yes	Yes	Yes	Yes		
	Depth (1-2')	2.7	2.7	Pass	Pass		
	Dimensional: Edge $\le 5'$ to TBC or 2' max	Yes	Fail	Yes	Fail		
	Outside Corners 2' from (projected) TBC	Yes	Yes	Yes	Yes		
	Gap between Brn. Multiple Panels ($\le 2'$, 0" preferred)	Yes	No	No	No		
	Clear Space (C)	Width x Walk and Outside Travel Lane	1.0%	1.0%	Pass	Pass	
	Slope Perpendicular to DWS ($\le 5.0\%$)	1.0%	1.0%	Pass	Pass		
	Slope Parallel to DWS ($\le 2.0\%$)	0.2%	0.2%	Fail	Fail		
Vertical Difference $\le 0.5'$ or 2:1 beveled	0.2%	0.2%	Yes	Yes			
Crosswalk (Marked or Unmarked)	Running Slope ($\le 5.0\%$)	1.1%	1.1%	Pass	Pass		
	Cross Slope* ($\le 2.0\%$)	6.7%	6.7%	Fail	Fail		
Push Button	Height above (T) ($42 \pm 2'$, or 36"-46" if RTE approved)	Pass	Pass	Pass	Pass		
	Offset from (T) ($\le 10'$, 18" max if RTE approved)	Pass	Pass	Pass	Pass		

Certified UDOT Inspector (Print): _____
 Certified Contractor (Print): _____

Suggested work to meet standards (Select all that apply):
 Re-grade intersection and/or roadway
 Widen roadway and/or pedestrian facilities
 Reconstruct adjacent sidewalk or pedestrian facility
 Purchase right-of-way (acquisition or temporary)
 Engr

After project inspection, file in ProjectWise and email to AD.Arramp@utah.gov and FHWA Area Engineer.

(b)

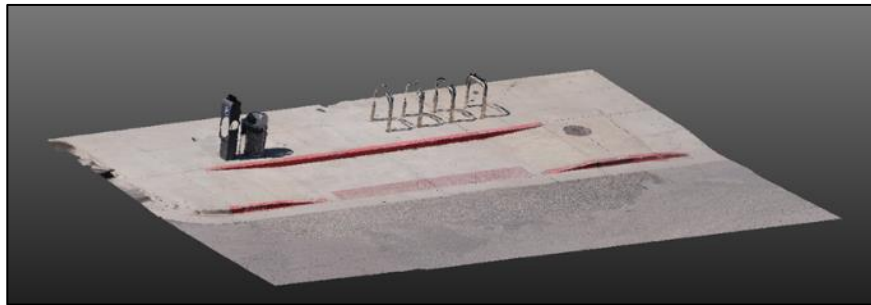
Measurement Comparison					
Element	LiDAR Based Measurements	Image-Based Measurements	UDOT's Measurement	Image-Based Error	LiDAR Based Error
PAR Left (cross)	1.61	0.83	2.10	1.27%	0.49%
PAR Right (Cross)	1.68	0.41	1.90	1.49%	0.22%
Turning space Running	1.94	1.66	1.60	0.06%	0.34%
Turning Space Cross	1.18	0.81	1.60	0.79%	0.42%
Ramp Running	0.98	0.33	0.80	0.47%	0.18%
Ramp Cross	0.34	0.63	0.20	0.43%	0.14%
Left Flare	20.3	22.3	53.0	30.75%	32.71%
Right Flare	16.4	16.1	16.5	0.39%	0.09%
Clear Space perp. To DWS	1.33	1.28	1.00	0.28%	0.33%
Clear Space para. To DWS	0.64	1.12	0.80	0.32%	0.16%
Crosswalk Running	1.62	1.92	1.40	0.52%	0.22%
Crosswalk Cross	1.05	1.34	0.70	0.64%	0.35%
Average Error				0.60%	0.27%

(c)

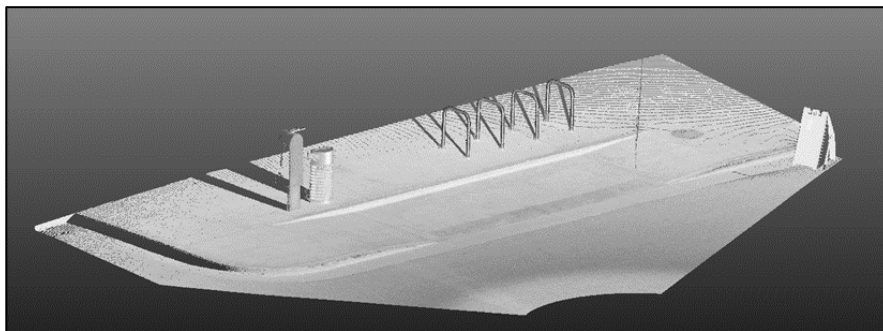
[Figure 18 – Comparison of UDOT’s in-field measurements to measurements extracted from image-based point clouds for Ramp 1. \(a\) & \(b\) UDOT C-170 evaluation form, \(c\) extracted measurements vs. UDOT’s measurements.](#)

4.4.2 Ramp 2

Ramp 2 is a pedestrian access ramp near the University (of Utah) Student Center. This ramp was chosen because it was built differently than the other access ramps in this project, yet the measurements are very accurate for this model as well. As you can see in Figure 20, the error between slopes extracted from the field and slopes extracted from the image-based point cloud model are 0.27%. The LiDAR error for this particular model was 0.19% (Figure 20 (c)). There were no outliers for this model and all extracted measurements were within a good range of the field measurements. The reason the LiDAR model is not shown in color is due to the fact that there was a heavy shadow cast over the ramp. While viewing this cloud with RGB colors, the ramp is shown very dark due to the shadow, which is why the model is shown in gray scale.



(a)



(b)

[Figure 19 – Ramp 2 point clouds using \(a\) photogrammetry and \(b\) LiDAR](#)

4.4.3 Ramp 3

Ramp 3 was another ramp near the university and was also chosen because of the different construction from other ramps in this portion of the project. Again, extracted measurements from the point clouds were very accurate, with an overall error of 0.28% for photogrammetry, and an error of 0.16% for LiDAR [Figure 22 (c)]. There were no problems with this access ramp's measurements and all extracted measurements were within an acceptable requirement to the in-field measurements. There was also a heavy shadow on this ramp, so the LiDAR model is shown in gray scale.

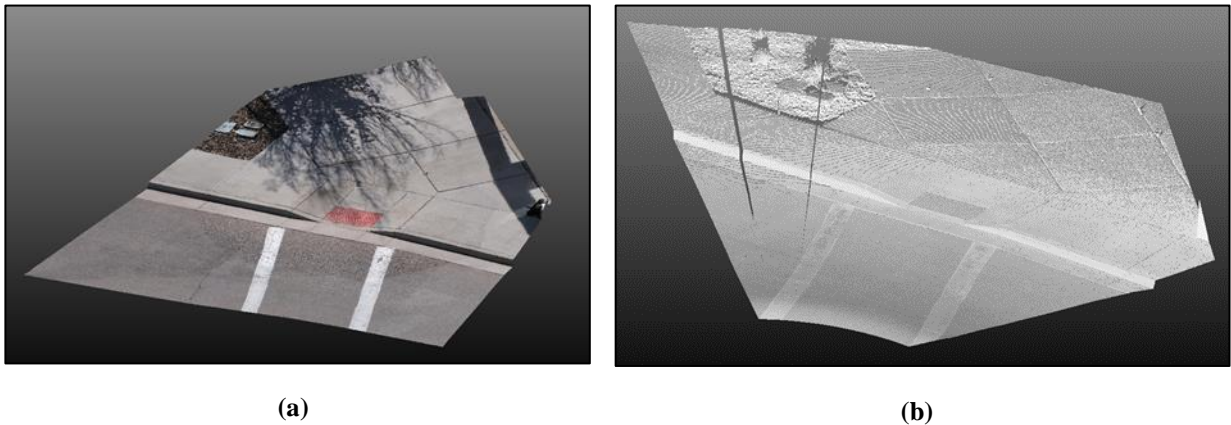


Figure 21 – Ramp 3 point clouds using (a) Photogrammetry and (b) LiDAR

[Figure 22 – Comparison of UDOT’s in-field measurements to measurements extracted from image-based point clouds for Ramp 3. \(a\) & \(b\) UDOT C-170 evaluation form, \(c\) extracted measurements vs. UDOT’s measurements.](#)

4.4.4 Ramp 4

Ramp 4, much like other access ramps in this project, was chosen because of its differing features and ramp components. This particular ramp had a higher overall error between in-field measurements and image-based point cloud measurements, however the error was still only 0.35%. The LiDAR point cloud is still consistent with an error of 0.19%. There are two measurements that could be considered outliers and those measurements are the flares of the pedestrian access ramp. However, as mentioned before, it is believed that the measurements from the point cloud are the more accurate measurements due to the accuracy of other extracted point cloud slopes. The smart level, too, was much too long to accurately measure the slope of each flare of the pedestrian ramp, and in-field measurements done with the Leica Disto D5 corroborated the measurements that were extracted from the point cloud.



(a)



(b)

Figure 23 – Ramp 4 point clouds using (a) Photogrammetry and (b) LiDAR

UDOT C-170 Pedestrian Access Evaluation Form
 Refer to UDOT's Form Standard Drawing for complete requirements
 March, 2020

Inspector: [Signature] Date: 3/12/20
 Primary: [Signature] Secondary: [Signature]

Notes:
 1. If a corner or location has multiple accesses, complete a separate form for each.
 2. Inventory access from the roadway facing with a 0.5% of clearance.
 3. Construction Release: All signs must be approved Technical Inspectability. Access will not fail due to substandard sidewalk.
 4. Document substandard sidewalks without an approved Technical Inspectability. Access will not fail due to substandard sidewalk.
 5. Work requests to adjust sidewalk cross slopes within at least one panel.
 6. Document substandard sidewalks without an approved Technical Inspectability. Access will not fail due to substandard sidewalk.
 7. Cross Slope Criteria: 0.5% Controlled by Slope/Type, 0.5% if Not Controlled by Slope/Type (including signals), Match Road Grade at Midblock

Access Type: Parallel, Multiple Overwalks, Corner, Access Location: NW, NE, SW, SE, S, E, W, N

Directional: Yes, No

Measurement and Determination (Per 911)

Item	Item (Pass Criteria)	Location	Location	Location	Location	Comments
Access	Grade Slope on Grade 0.5%	Pass	Fail	Pass	Pass	Grade Slope on Grade 0.5%
Pedestrian Access Route (PAR)	Width (4.4 ft)	Pass	Pass	Pass	Pass	Width (4.4 ft)
Turning Space (T)	Running Space (1.8 ft)	Pass	Pass	Pass	Pass	Running Space (1.8 ft)
Ramp (R)	Grade Slope (1.2%)	Pass	Pass	Pass	Pass	Grade Slope (1.2%)
Flares (F1/F2)	F1 Slope (0.5%)	Pass	Pass	Pass	Pass	F1 Slope (0.5%)
Abutment Access (A)	Grade Slope (0.5%)	Pass	Pass	Pass	Pass	Grade Slope (0.5%)
Cut Through Island (CI)	PAR Width (5.0 ft)	Pass	Pass	Pass	Pass	PAR Width (5.0 ft)

(a)

Element	Item (Pass Criteria)	Location	Location	Location	Location	Comments
Dreadable Walking Surface (DWS)	Color Contrasts with Surrounding Surface	Yes	Yes	Yes	Yes	
	Spots Fall Curb Cut (2' x 4' height, 2" or shall)	Yes	Yes	Yes	Yes	
	Directional Edge 0.5" to 1" to 2" or shall	Yes	Yes	Yes	Yes	
	Chicote Corners 2" from [detected] TIC	Yes	Yes	Yes	Yes	
	Gap Between Item Multiple Panels (2' x 2' or perforated)	Yes	Yes	Yes	Yes	
Clear Space (C)	Within 4' Walk and Curbside Travel Lane	Pass	Pass	Pass	Pass	
	Slope Perpendicular to DWS (±5.0%)	Pass	Pass	Pass	Pass	
	Slope Parallel to DWS (±2.0%)	Pass	Pass	Pass	Pass	
Crosswalk (Marked or Unmarked)	Running Slope (±5.0%)	Pass	Pass	Pass	Pass	
	Cross Slope (±2.0%)	Pass	Pass	Pass	Pass	
Push Push	Height above (1) (42" or 30" or 40" if RTE approved)	Pass	Pass	Pass	Pass	
	Offset from (1) (1.0, 3.0, 5.0' max & RTE approved)	Pass	Pass	Pass	Pass	

Certified UDOT Inspector (Print):
 Certified Contractor (Print):

Suggested work to meet standards (Select all that apply):
 Re grade intersection and/or roadway
 Widen roadway and/or pedestrian facilities
 Reconstruct adjacent sidewalk or pedestrian facility
 Purchase right of way (acquisition or temporary)
 Other

After project inspection, file in ProjectWise and email to ADGramps@utah.gov and FHWA Area Engineer.

(b)

Comparison of Slopes					
Element	LiDAR-Based Measurements	Image-Based Measurements	UDOT's Measurement	Image-Based	LiDAR-Based
PAR right cross	0.98	1.28	1	0.28%	0.02%
Turning space running	1.76	2.08	1.8	0.28%	0.04%
turning space cross	3.00	3.01	2.8	0.21%	0.20%
Ramp Running	7.98	7.77	7.4	0.37%	0.58%
Ramp cross	1.18	1.46	1.3	0.16%	0.12%
F2 Slope	21.3	22.3	19	3.30%	2.26%
F1 Slope	21.8	21.8	19.3	2.53%	2.53%
Clear space Perp. To DWS	1.24	1.91	1.50	0.41%	0.26%
Clear space Paral. To DWS	0.29	0.88	0.50	0.38%	0.21%
Crosswalk running	1.49	1.12	1.70	0.58%	0.21%
Crosswalk cross	1.21	0.84	1.30	0.46%	0.09%
Average				0.35%	0.19%

(c)

Figure 24 – Comparison of UDOT's in-field measurements to measurements extracted from image-based point clouds for Ramp 4. (a) & (b) UDOT C-170 evaluation form, (c) extracted measurements vs. UDOT's measurements.

4.4.5 Ramp 5

Pedestrian Ramp 5, much like the other ramps, also has a very high accuracy of measurements. The overall error for the image-based reconstructed point cloud is 0.24%. The LiDAR-reconstructed point cloud has an even lower error percentage of 0.18. Pedestrian access ramp 5 does not have a UDOT C-170 evaluation form due to the fact that the final two ramps, ramps 5 and 6, were not done with UDOT representatives. However, in-field evaluations were still carried out using the UDOT C-170 procedures, but instead of a Smart Level, in-field measurements were done with a Leica Disto D-5 measuring tool to measure slopes.



(a)



(b)

Comparison of Slopes					
Element	LiDAR-Based Measurements	Image-Based Measurements	Leica Disto D5 Measurements	Image-Based Error	LiDAR-Based Error
Par Left Cross	1.39	1.84	1.25	0.59%	0.14%
Par Right Cross	0.93	0.18	0.5	0.32%	0.43%
Turning Running	2.32	2.92	2.58	0.34%	0.26%
Turning Cross	1.73	2.08	1.94	0.14%	0.21%
Ramp Running	5.14	5.06	4.96	0.10%	0.18%
Ramp Cross	2.1	2.0	2.15	0.14%	0.07%
Left Flare	8.62	8.09	8.36	0.27%	0.26%
Right Flare	3.21	3.17	3.29	0.12%	0.08%
Clear Space Perp	2.25	1.92	2.10	0.18%	0.15%
Clear Space Paral.	2.63	2.47	2.83	0.36%	0.20%
Cross Running	2.35	2.39	2.16	0.23%	0.19%
Cross Cross	0.58	0.56	0.60	0.04%	0.02%
Average				0.24%	0.18%

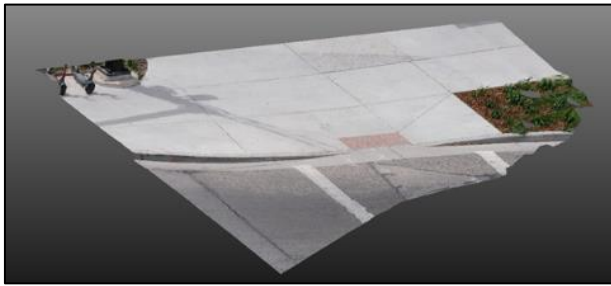
(c)

Figure 25 – Ramp 5 point clouds using (a) Photogrammetry and (b) LiDAR. (c) Point cloud measurements

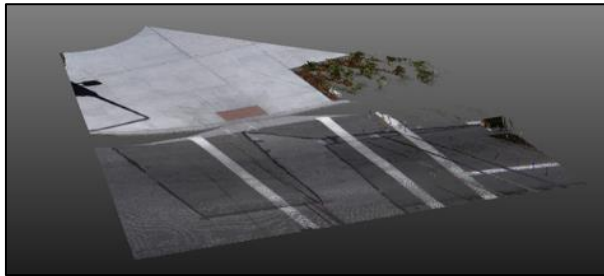
4.4.6 Ramp 6

Ramp 6 is no different than the other models in that both photogrammetry and LiDAR presented low margins of error. The image-based point cloud had an overall error of 0.17%, and the LiDAR-based model had an overall error of 0.14%. This ramp was also inspected without

UDOT representatives, but the inspections were carried out in accordance with UDOT C-170 standard procedures.



(a)



(b)

Comparison of Slopes					
Element	LiDAR-Based Measurements	Image-Based Measurements	Leica Disto D5 Measurements	Image-Based Error	LiDAR-Based Error
Par Cross Left	1.51	1.34	1.42	0.08%	0.09%
Par Cross Right	1.80	1.45	1.60	0.15%	0.20%
Turning Running	1.71	1.74	1.68	0.06%	0.03%
Turning Cross	1.10	1.11	0.95	0.16%	0.15%
Ramp Center running	4.17	4.24	4.18	0.06%	0.01%
Ramp center cross	1.49	1.58	1.34	0.24%	0.15%
Left Flare	5.70	5.53	5.60	0.07%	0.10%
Right Flare	5.23	5.16	5.32	0.16%	0.09%
Clear space perp to DWS	3.85	3.97	3.90	0.07%	0.05%
Clear space paral. To DWS	1.67	2.54	2.08	0.46%	0.41%
Crosswalk Running	0.09	0.06	0.45	0.39%	0.36%
Crosswalk Cross	1.47	1.41	1.50	0.09%	0.03%
Average				0.17%	0.14%

(c)

Figure 26 – Ramp 6 point clouds using (a) Photogrammetry and (b) LiDAR. (c) Point cloud measurements

4.5 Summary

For both case studies presented in this research report, image-based and LiDAR-based reconstructed point clouds both presented very accurate and comparable data. For asset management, the overall reconstructed sign error for image-based point clouds was 4.33%, with an overall average sign density of 29 points per square inch. The standard deviation and coefficient of variations were 14.6 and 0.49, respectively. For LiDAR-based reconstruction, the overall reconstructed sign error was 3.48%, with an overall sign density of 0.96 points per square inch. The standard deviation and coefficient of variation were 0.41 and 0.42, respectively. Both technologies were very similar in terms of reconstructed sign errors, having a difference of less

than 1% error. The image-based point clouds were much more dense than the LiDAR-based point clouds, but this is most likely due to the fact that Mandli Communications limits the amount of data gathered due to the sheer amount of data gathered and transferred. The standard deviations and coefficients of variation point to the fact that the LiDAR point clouds are slightly more uniform when it comes to point cloud density. The lower the coefficient of variation, the less variability the point cloud has in density. Since image-based reconstruction has a coefficient of variation of 0.49, and LiDAR has a CV of 0.42, the LiDAR point clouds are slightly more uniform.

For the pedestrian access case study, both technologies are very comparable in terms of measurement errors. The errors were measured from how much the point cloud-extracted measurement deviated from the measurements that were extracted in the field. The overall error for image-based reconstruction is 0.32%, with a standard deviation of 0.15 and a coefficient of variation of 0.48. For LiDAR-reconstructed point clouds, the overall error is 0.19%, with a standard deviation of 0.04 and a coefficient of variation of 0.24. Much like the asset management case study, LiDAR technology was more accurate and the measurements had more uniformity in terms of how much they deviated from the extracted in-field measurements. Nevertheless, the image-based point clouds were still highly accurate, with an error percentage of only 0.13% higher than LiDAR-based point clouds.

5.0 CONCLUSIONS

5.1 Summary

It is imperative for transportation facility managers to have up-to-date knowledge of the current state of all assets in various areas of their departments. For an individual to know the current status of all assets, there must be an efficient, accurate method of data collection and evaluation so that managers can accurately plan and implement necessary procedures to take care of poor assets. There are some technologies being used such as LiDAR to manage these assets currently, however, LiDAR is a very expensive and involved technology that requires special

knowledge and operators to gather and interpret data. Image-based 3D reconstruction (i.e., photogrammetry) is a much cheaper and simpler alternative to LiDAR, that provides similar data outputs in the form of 3D point clouds. The objectives of this research project were to compare image-based reconstructed point clouds to LiDAR points clouds to see if photogrammetry can be used as an acceptable alternative to the currently used LiDAR technology. While photogrammetry may be subject to slightly less accurate data, the ease of use, low cost, and high functionality of image-based reconstruction technologies far outweighs the slight drop in point cloud accuracies.

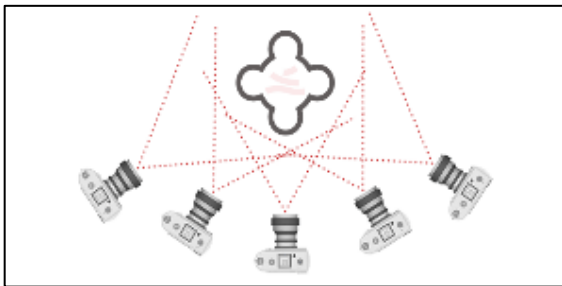
Data was gathered in two separate case studies, with each study being slightly different from the other in terms of data collection and data evaluation. The first case study was asset management of roadways with an emphasis on highway data collections. For this procedure, a camera capable of capturing high resolution videos at high frame rates was mounted to the hood of a vehicle using a suction cup mount, and data was collected while driving around various areas of city streets and highways around Salt Lake City. The second case study was focused on pedestrian access ramp evaluations. For this study, images were captured in a circular pattern around various pedestrian access ramps and uploaded into 3D reconstruction softwares for processing and evaluation.

Data was also evaluated differently in each case study that is specific to the type of data gathered and processed. For asset management, evaluations were carried out by comparing reconstructed sign size ratios (height to width), to the actual size of the sign in the real world. The purpose of this comparison was to see how accurately objects are generated in image-based and LiDAR-based point clouds. For pedestrian access ramps, data was evaluated by extracting slope measurements from various access ramp components, and comparing the LiDAR-based and image-based measurements to the measurements that were extracted during an in-field evaluation done according to the UDOT C-170 Pedestrian Access Ramp Evaluation form. Along with the unique case-specific evaluations, evaluations of point cloud density for each case study were conducted. Various density measurements were extracted; however, the most important density variable is the number-of-neighbors calculation. The number-of-neighbors density calculation gives a comprehensive overview of the density of a point cloud. This characteristic is calculated by defining a circle with a user-chosen radius, and the program then imposes circles of

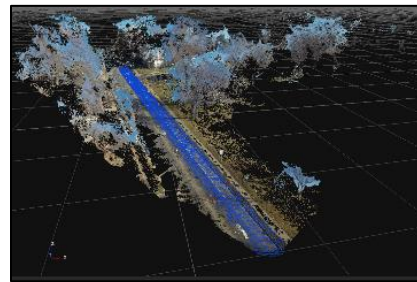
the given radius throughout all areas of the point cloud. The final density output defines the total number of 3D points inside each user-defined circle throughout various areas of the point clouds, so the viewer has a comprehensive idea of how the density varies in different areas. The research presented in this report points to the fact that photogrammetry could most definitely be used for transportation purposes and provide a high quality and accurate point cloud model. The small amount of accuracy sacrificed by using photogrammetry is far outweighed by the low cost and ease of use.

5.2 Limitations and Challenges

There were a few noticeable challenges encountered while conducting this research, and the technology was found to have some minor limitations. The first challenge encountered during this research project was finding a photogrammetry software that would process the sequential images from asset management data collections. As previously mentioned and shown in Figure 27 (a) below, images should be acquired in a circular pattern with sufficient overlap between images for an accurate 3D model. Images acquired during data collections were captured in a linear pattern, as shown in Figure 27 (b). Linear images were tested in Reality Capture, Agisoft, 3DF Zephyr, Pix4D, and Context Capture to see which program would provide the best model. Context Capture provided the most consistent and clear 3D models, so the rest of the research study was carried out using Context Capture as the main cloud processing software.



(a)



(b)

Figure 27 – Image acquisition pattern. (a) Recommended capture procedure and photo overlap, (b) Pattern of photo overlap and image acquisition pattern during asset management data collection. The blue linear objects in photo (b) are the extracted positions of extracted frames.

Another challenge encountered while conducting asset management research was finding the most opportune time to collect data due to environmental conditions. Photogrammetry softwares can be sensitive to reflective surfaces in images. Factors such as snow, rain, sunlight, and car reflections can cause problems with reconstruction. If there is too much sunlight during data collections, the light may reflect off of various objects such as vehicles, items in the road, and highway signs. These conditions were usually encountered during days with no cloud cover, and the sun shining from behind the vehicle of travel. It is best to collect data on sunny days with intermittent cloud cover to prevent constant direct sunlight. Factors such as rain and snow can also be an issue. Utah does not get as much rain as other states, however snow can be a problem. During periods of heavy snow, it is difficult to collect good data because of the snow on the shoulders of roadways. Even when a road is plowed, there is still a lot of snow surrounding the roadway and landscape surfaces, which can cause too much reflection in images leading to a poor 3D model.

One of the biggest limitations of asset management data collections using photogrammetry is the speed that one is able to travel and still acquire good data. During this research, it was concluded that videos gathered while traveling greater than 50 miles per hour were not able to be processed. One of the most important aspects of image alignment during photogrammetry reconstruction is having enough keypoints in each image to be able to have an accurate alignment. As you can see in the following Figure 28, keypoint alignment is best between 10-30 miles per hour. Good models were attainable at speeds greater than 40 miles per hour, however image alignment was much more difficult. Above 50 miles per hour, image alignment was unsuccessful, therefore a 3D point cloud model could not be created. A keypoint analysis was done using speeds from less than ten miles per hour, to a speed of 40 miles per hour. With the exception of location one, the total number of keypoints decreases as speed increases [Appendix A, Figure 36]. This is believed to be the reason for poor image alignment while going faster than 50 miles per hour.

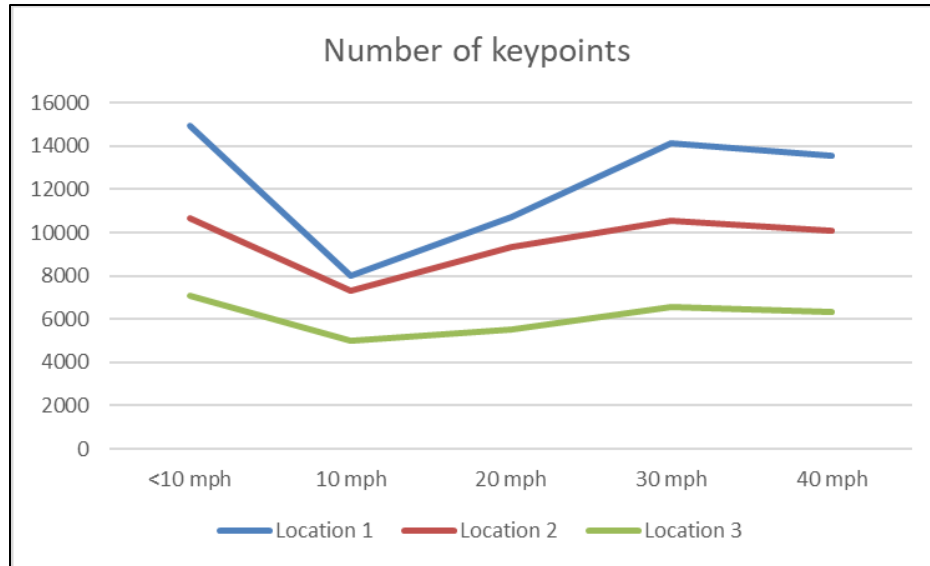


Figure 28 – Number of keypoints of 3 locations according to data acquisition speed.

Along with the speed limitation comes the challenge of being able to travel at a lower rate of speed on a highway. Most highway speeds are around 65-70 miles per hour, so it is imperative to collect data during low traffic hours. High amounts of traffic can cause obstructions in the extracted images which may lead to failed data processing, not to mention it can be dangerous to drive slower than the flow of traffic. The most effective time to collect data was between 9 a.m. and 1 p.m. on weekdays, and weekend afternoons. This allowed for slower travel on the roadways with less chance of interrupting traffic or causing a collision.

6.0 RECOMMENDATIONS AND IMPLEMENTATION

6.1 Recommendations

There are a few key recommendations in order to make data collection and processing a more streamlined process. The first recommendation for asset management data collection is to pay close attention to the time of day and lighting conditions. If it is earlier in the day and the sun is rising from the east, it is best to collect data driving west to ensure that assets are adequately illuminated, and the sun is not shining directly into the camera sensor. Likewise, later in the afternoon as the sun is setting to the west, it is best to collect data driving east for the same

reason. Another factor to keep in mind while collecting data is the speed of travel. Though satisfactory results are achievable up to 50 MPH, it is best to travel as slow as possible during data collection to ensure the camera sensor is gathering the most amount of data possible. One factor that must be handled while driving slower speeds during data collections is the fact that the more data the sensor is gathering, the more robust the point cloud will be, leading to large file sizes. In order to combat storage requirement problems during post-processing, down-sampling should be used to ensure that file sizes do not get too large. As can be seen in Table 15 below, most point clouds can be down-sampled by 75% while retaining data accuracy and visual representations. High-density point clouds are good, but one has to ask the question ‘how much data is too much?’ The point clouds before down-sampling were very good quality, but even when down-sampled by 75%, the point clouds still retained the high accuracy and visual characteristics of the non-down-sampled point clouds.

Table 15 – Effect of down-sampling on point cloud quality

Effects of down sampling on file size and sign visibility					
Model		down sampling percentage			
		100%	75%	50%	25%
Model 1	# of Points	351,960,833	263,970,625	175,980,417	87,990,208
	File Size	11.1 GB	8.84 GB	5.89 GB	2.94 GB
	Visibility	Great	Great	Good	Good
Model 2	# of Points	318,014,773	238,511,080	159,007,387	79,503,693
	File Size	10 GB	7.99 GB	5.33 GB	2.66 GB
	Visibility	Great	Great	Good	Good
Model 3	# of Points	770,930,961	578,198,221	385,465,481	192,732,740
	File Size	24.4 GB	19.3	12.9 GB	6.46 GB
	Visibility	Great	Good	Good	Fair
Model 4	# of Points	714,905,162	536,178,872	357,452,581	178,726,291
	File Size	22.6 GB	17.9 GB	11.9 GB	5.99 GB
	Visibility	Good	Good	Fair	Fair
Model 5	# of Points	570,359,305	427,769,479	285,179,653	142,589,826
	File Size	19.1 GB	14.3 GB	9.56 GB	4.78 GB
	Visibility	Good	Good	Fair	Poor
Model 6	# of Points	500,000,000	375,000,000	250,000,000	125,000,000
	File Size	16.7 GB	12.5 GB	8.38 GB	4.19 GB
	Visibility	Great	Good	Good	Fair

In order for one to decide which technology would work best for their case, they need to decide what is necessary when using these technologies for virtual reconstruction, as both have strengths and weaknesses. Image-based reconstruction can be a very useful technology for lapses in model generation. For example, if the contracted LiDAR company scans a state's roadways every two years, it is very likely that there will be gaps in updated models such as when a roadway has undergone construction, assets are added/changed, or a traffic accident causes changes to a roadway. It would be very simple for an individual to go out and collect data on these changed roadway sections rather than outsourcing a company to come back and scan just a few areas around the state. Also, in-field data storage is another advantage of image-based reconstruction. The camera that was used for the asset management portion of this research stores all collected data on a small micro SD (Secure Digital) card that is capable of storing large amounts of data on a small chip. The current LiDAR asset management approach requires the LiDAR company to physically mail a large amount of data on hard drives to processing offices in order to transfer data in the most efficient way possible. Although this may be okay in some cases, the process of physically mailing hard drives can be tedious and time-consuming. Another factor to consider is point cloud density. The denser a point cloud is, the larger the file size is, requiring more storage in the office. As mentioned previously, Mandli most likely uses technologies to limit the amount of data captured to ensure they have sufficient data without having too many unnecessary points. The only way to limit the amount of data the GoPro captures is by changing the resolution. 2.7K resolution has a high density of pixels, making the point cloud model very dense. The image-based point clouds require a larger amount of storage in the office; however, point clouds can be down-sampled without losing data accuracy in order to optimize data storage requirements in the office. Again, it depends on the needs of the individual requiring these point clouds, and careful consideration must be taken when deciding how much data is the most optimal to achieve the desired results. Both technologies are very useful, and each has a place during highway reconstruction and asset management.

The pedestrian access ramp case study was a very straightforward case study with very limited problems encountered. The main factors to consider while collecting pedestrian access ramp data varies between each technology. For image-based reconstruction, the most important factor is to ensure that each image has sufficient overlap with the previous and following image. If images do not have sufficient overlap, the point cloud processing software will struggle to align

all images and create a dense and accurate point cloud. For LiDAR data collections, it is important to ensure that the LiDAR scanner is exactly level before carrying out scanning procedures to ensure that the reconstructed point cloud is level with the horizon so that extracted slope measurements are as accurate as possible.

6.2 Implementation Plan

This implementation plan has been written in accordance with the information presented in this report. It is assumed that all technology used is the same technology presented previously in the paper.

6.2.1 Asset Management Implementation

1. Choose the optimal time of day for data collection. Driving west is better early in the day etc.
2. Mount the camera to the hood of the vehicle ensuring that the field of view can capture all side and overhead signs while omitting parts of the vehicle from the FOV (see below).

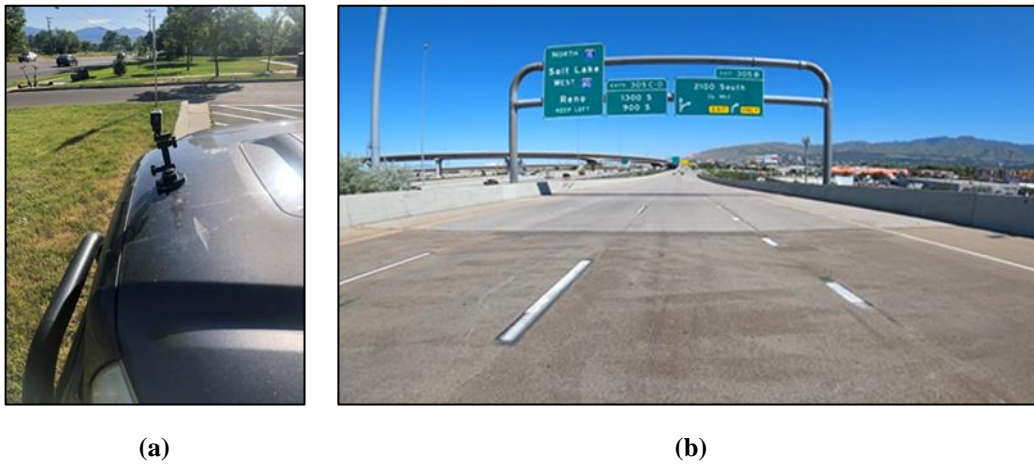


Figure 29 – (a) camera mounting area and (b) field of view for a hood-mounted camera

3. Ensure that the correct video settings are selected before beginning data collections. A 2.7k video resolution at 120 frames per second is recommended.

4. Begin recording video before the section of interest to ensure that the camera has enough time to begin recording and not miss any data. It is important to try and travel as slow as possible during this step to ensure that the most amount of data possible is captured.
5. Once the section of interest has been recorded, analyze the video to ensure that all pertinent data has been captured before returning to the office for post-processing.
6. Once all data has been gathered and appears to be satisfactory, return to the office and begin post-processing. The following steps are assuming Context Capture is used as the default cloud processing console.
7. Begin a new project in context capture and save it to the desired locations.
8. Import the recorded video into the Context Capture software and select the desired number of frames to be extracted. You can specify the start time and end time of the extracted frames, as well as the frequency of extracted frames. Even though video was recorded in 120 FPS, photos were extracted every 0.02 seconds (50 FPS), and then increased to 0.015 (66 FPS) if the first iteration failed. The largest number of extracted frames used is 0.01 (100 FPS), to ensure the system isn't overloaded during processing.

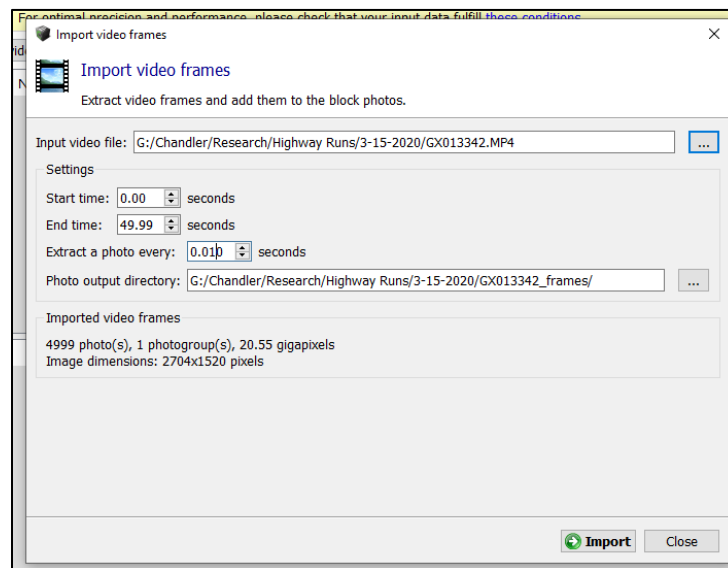


Figure 30 – Video frame extraction window

9. For some cameras, the software will recognize the focal length and sensor size, however, it did not recognize the GoPro Hero 8 sensor size and focal length. The focal length is 2.92mm and the sensor size is 6.17mm. For Context Capture, only the width value of the sensor size is used.

10. Submit the images for aerotriangulation (image alignment). This step is where ground control points can be input if there are such points. In the aerotriangulation settings tab (shown below), there are a few key parameters to change. Keypoint density can be kept as normal, however, if the first few iterations fail, the density can be changed to ‘high’. Next, change the pair selection mode to sequence. Since the images from the video are extracted in a sequential manner, sequence selection mode allows the program to go sequentially through the images for matching. The maximal distance should be set anywhere from 3-6. It is best to start at 3 and go up from there if the triangulation is not satisfactory. Component construction mode should be set to multi-pass to allow the program numerous passes through the images for matching. Aerotriangulation can be an iterative process requiring numerous submissions before an acceptable model is generated. If aerotriangulation fails or is not satisfactory, it is best to adjust these parameters slightly before resubmitting image alignment. This step can be a trial-and-error process.

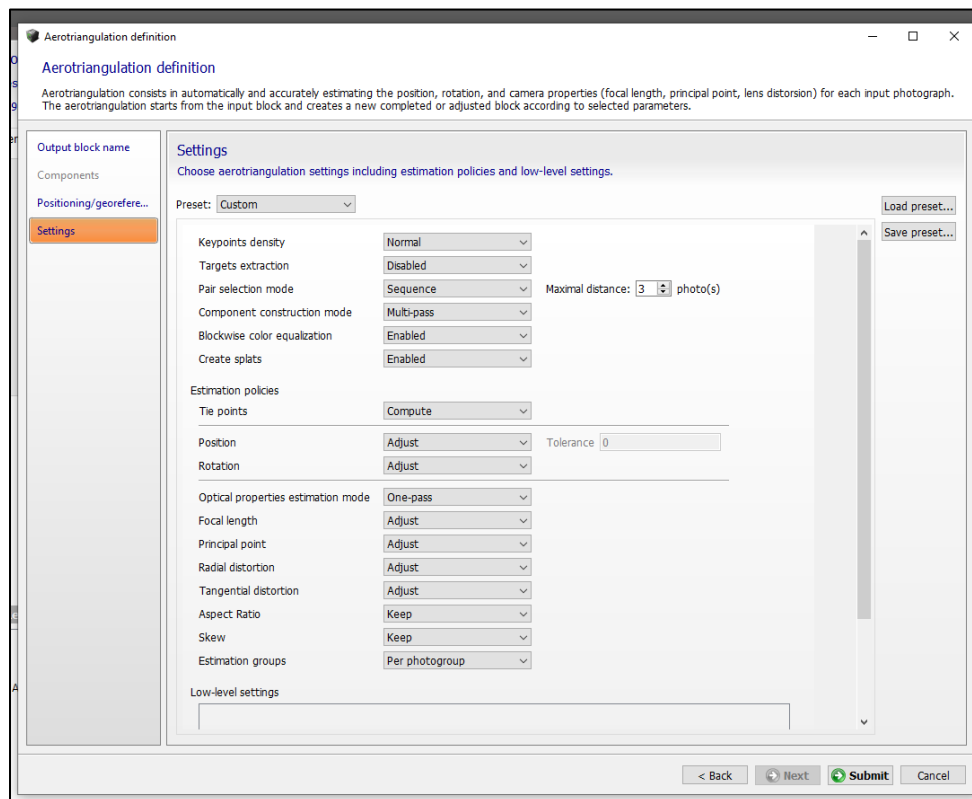


Figure 31 – Aerotriangulation Settings

11. Once image alignment is complete, submit a new 3D reconstruction. Depending on the processing power of the computer being used, an error such as the one below may be encountered.

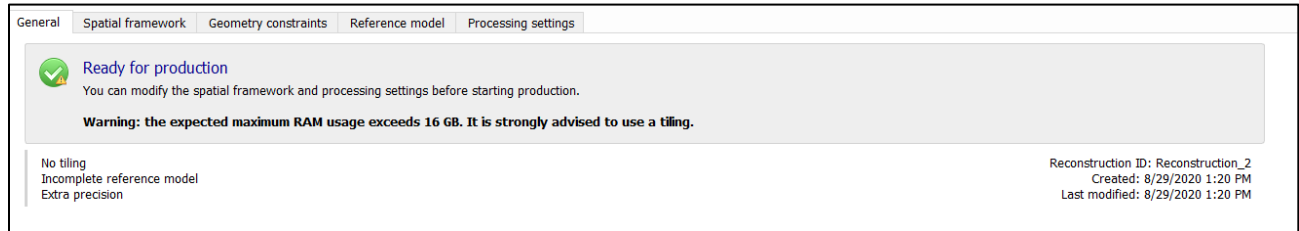


Figure 32 – Maximum RAM usage exceeded warning

If this error is encountered, go into the spatial framework tab and change the mode to ‘adaptive tiling’. This splits the model into a number of different tiles for separate processing to make the processing easier on the computer.

12. Once the tiling step has been completed, it is time to submit the model for processing. Choose ‘submit a new production’. Name the model and select the output location, and in the ‘purpose’ tab, select 3D point cloud. The rest of the tabs can stay as they are. Choose your export destination and submit the new production.
13. Once the point cloud is done processing, we recommend opening it in Cloud Compare for viewing and measurement extractions. Cloud Compare is an open-source cloud viewing and processing software that is easy to use and has handled these point clouds very well.

6.2.2 Pedestrian Access Ramp Implementation

1. The first step is choosing an optimal time of the day to gather data on a pedestrian access ramp that will limit the number of pedestrians passing through the scene. People can be removed in post-processing, but limiting the amount of people in the scene limits the amount of cleanup that needs to be done later.
2. For LiDAR: Upon arriving on the scene, ensure the LiDAR scanner is perfectly level and locked to the tripod before doing any scanning procedures.
For Photogrammetry: Ensure that the camera settings are set to capture high-quality images with a large number of pixels. JPEG images with a size of 6240x4160 pixels were used in this study.

3. For LiDAR: Once the scanner is level, choose the appropriate settings for the scene and environmental conditions. Scans were done on sunny days, so the “bright” environmental setting was used, and density number 8 was used (the second highest density the scanner offers). If you have the option to view the scene before scanning, ensure that all pertinent ramp components are captured fully in the scene.
4. For LiDAR: Begin scanning the scene. Once the LiDAR scanner begins scanning, there is no need to do anything else. Let the scanner finish its process before touching or moving the scanner.

For Photogrammetry: Begin capturing images in a circular motion around the ramp. Ensure that each image has sufficient overlap between the previous and following images. It is imperative to ensure that each point in the scene is captured in at least 3 separate images to ensure the images have sufficient overlap for the image alignment process.

5. For LiDAR: Once scanning has completed, if you have the option to view the point cloud, take a look at it and ensure that all details have been captured. If you are not satisfied, adjust the scanning parameters and scan the scene again.

For Photogrammetry: Once all images have been captured, review each image to ensure that there is sufficient overlap between images and all ramp components have been captured. If the images look good, it is time to return to the office for post-processing.

6. The following steps will only apply to photogrammetry. Since the LiDAR scanner generates the point cloud during the scanning process, there is no need for any post-processing other than cleaning noise from the scene that may have been caused by pedestrians or vehicles.
7. Once you are back at the office, upload all captured images into the Context Capture software. Since a high-quality DSLR camera was used for these images, Context Capture automatically recognized the FujiFilm XT-30 sensor size and focal lengths.
8. Submit the photo group for aerotriangulation. Keep all settings the same in the settings tab except for ‘component construction mode’. Choose ‘Multi-Pass’ to ensure the program makes multiple passes through the images to have the most accurate image alignment possible.
9. Once all images have been successfully aligned, submit the aligned images for a new production. Choose 3D point cloud as the output, and use adaptive tiling for large models.

All pedestrian access ramps were significantly smaller in size than the asset management point clouds, so no adaptive tiling was needed.

10. Submit the model for 3D point cloud production.
11. Once the production has completed, open the point cloud in Cloud Compare and ensure that the final product is satisfactory before carrying out measurements.

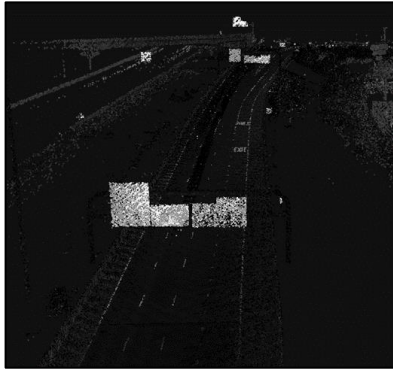
REFERENCES

- [1] “Public Road and Street Mileage in the United States by Type of Surface” [Online]. National Transportation Statistics, Table 1-4. Bureau of Transportation Statistics.
- [2] Mandli, “Utah DOT: The Blueprint,” 2012. [Online]. Available:
<https://www.mandli.com/wp-content/uploads/2016/02/Utah-DOT-Blueprint.pdf>.
- [3] S. Gordon, D. D. Lichti, M. P. Stewart, and M. Tsakiri, “Metric performance of a high-resolution laser scanner,” in *Videometrics and Optical Methods for 3D Shape Measurement*, 2000, vol. 4309, pp. 174–184.
- [4] C. Tucker, “Testing and verification of the accuracy of 3D laser scanning data,” in *Symposium on geospatial theory, Processing and Applications, Ottawa*, 2002.
- [5] J. Clark and S. Robson, “Accuracy of measurements made with a Cyrax 2500 laser scanner against surfaces of known colour,” *Surv. Rev.*, vol. 37, no. 294, pp. 626–638, 2004.
- [6] D. D. Lichti and B. R. Harvey, “The effects of reflecting surface material properties on time-of-flight laser scanner measurements,” *tc*, vol. 2, p. 1, 2002.
- [7] T. Voegtle and S. Wakaluk, “Effects on the measurements of the terrestrial laser scanner HDS 6000 (Leica) caused by different object materials,” *Proc. ISPRS Work*, vol. 38, no. 2009, pp. 68–74, 2009.
- [8] Z. Zhou, J. Gong, and M. Guo, “Image-based 3D reconstruction for posthurricane residential building damage assessment,” *J. Comput. Civ. Eng.*, vol. 30, no. 2, p. 4015015, 2016.
- [9] A. Bhatla, S. Y. Choe, O. Fierro, and F. Leite, “Evaluation of accuracy of as-built 3D modeling from photos taken by handheld digital cameras,” *Autom. Constr.*, vol. 28, pp. 116–127, 2012.
- [10] H. Fathi, F. Dai, and M. Lourakis, “Automated as-built 3D reconstruction of civil infrastructure using computer vision: Achievements, opportunities, and challenges,” *Adv. Eng. Informatics*, vol. 29, no. 2, pp. 149–161, 2015.
- [11] L. Klein, N. Li, and B. Becerik-Gerber, “Imaged-based verification of as-built documentation of operational buildings,” *Autom. Constr.*, vol. 21, pp. 161–171, 2012.
- [12] M. Pollefeys *et al.*, “Detailed real-time urban 3d reconstruction from video,” *Int. J. Comput. Vis.*, vol. 78, no. 2–3, pp. 143–167, 2008.
- [13] I. Brilakis, H. Fathi, and A. Rashidi, “Progressive 3D reconstruction of infrastructure with

- videogrammetry,” *Autom. Constr.*, vol. 20, no. 7, pp. 884–895, 2011.
- [14] A. Rashidi, F. Dai, I. Brilakis, and P. Vela, “Optimized selection of key frames for monocular videogrammetric surveying of civil infrastructure,” *Adv. Eng. Informatics*, vol. 27, no. 2, pp. 270–282, 2013.
- [15] M. Lato, M. Diederichs, “Mapping Shotcrete Thickness using LiDAR and Photogrammetry Data: Correcting for Over-Calculation due to Rockmass Convergence.” 2014.
- [16] D. Veneziano, R. Souleyrette, S. Hallmark, “Integrating LiDAR and Photogrammetry in Highway Location and Design.” 2003.
- [17] L. Klein, N. Li, and B. Becerik-Gerber, “Imaged-based verification of as-built documentation of operational buildings,” *Autom. Constr.*, vol. 21, pp. 161–171, 2012.
- [18] S. Chae and N. Kano, “Application of location information by stereo camera images to project progress monitoring,” in *Proceedings of the 24th International Symposium on Automation and Robotics in Construction*, Kochi, Kerala, India, 2007, pp. 19–21.
- [19] Dai, F., Rashidi, A., Brilakis, I., & Vela, P. (2013). Comparison of image-based and time-of-flight-based technologies for three-dimensional reconstruction of infrastructure. *Journal of construction engineering and management*, 139(1), 69-79.
- [20] Popescu, C., Täljsten, B., Blanksvärd, T., & Elfgren, L. (2019). 3D reconstruction of existing concrete bridges using optical methods. *Structure and Infrastructure Engineering*, 15(7), 912-924.

APPENDIX A: SUPPLEMENTARY MATERIAL

The following images in this appendix are supplemental material.



(a)



(b)

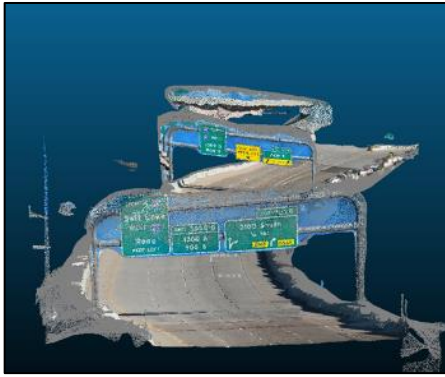


(c)



(d)

[Figure 33 – Sample of highway asset management point cloud using LiDAR](#)



(a)



(b)



(c)



(d)

Figure 34 – Sample of highway asset management point cloud using photogrammetry

Table 16 – Technology and equipment comparison

Case Study	Technology	Equipment	Cost of Equipment	Software	Cost of Software	In-Field Labor	In-Field Data Storage Requirements	Office Data Storage Requirements
Vehicular Systems for Asset Management	Photogrammetry	GoPro Hero 8 Black Edition	\$400	Context Capture	\$9,100 (First year) +\$1100 (yearly)	5 min equipment setup + 0.04 Man-hr/mi	~0.5 GB/Mi (2.7K @ 120 FPS)	~15 GB/Mi
				3DF Zephyr	\$149 (Lite) \$3,200 (Pro) \$4,200 (Aerial) (Perpetual)			
	LiDAR	2 * Velodyne HDL-32 (x2)	\$49,000 (for two)	Roadview Workstation	Comes with Mandli Communication services	1 hr equipment setup + 0.036 Man-hr/mi	~3 Gb/Mi	~3 Gb/Mi
Unmanned Aerial Systems for Asset Management	Photogrammetry	DJI Mavic 2 Pro	\$1600	Pix4D	\$4,990 (Perpetual)	0.5 hr equipment setup + 0.4 Man-hr/Mi	~0.5 GB/Mi	~2.7 GB/Mi
	LiDAR	DJI M600 with VX15 LiDAR Scanner	\$6000 (Drone) \$140,000 (VX15)	Pix4D	\$4,990 (Perpetual)	0.5 hr equipment setup + 0.53 Man-hr/Mi	~1 GB/Mi	~1 GB/Mi
Pedestrian Access Ramp	Photogrammetry	Fujifilm XT-30 (18-55mm lens)	\$1300	Context Capture	See above	0.08 Man-hr/Ramp	300 Mb/Ramp (30 images, 6240x4160)	7.5 GB/Ramp
				3DF Zephyr	See above			
	LiDAR	Maptek I-Site 8820	\$30,000 (Used)	Maptek PointStudio	Included with the purchase of the scanner	0.25 Man-hr/Ramp	545 Mb/Ramp	545 Mb/Ramp



(a)



(b)

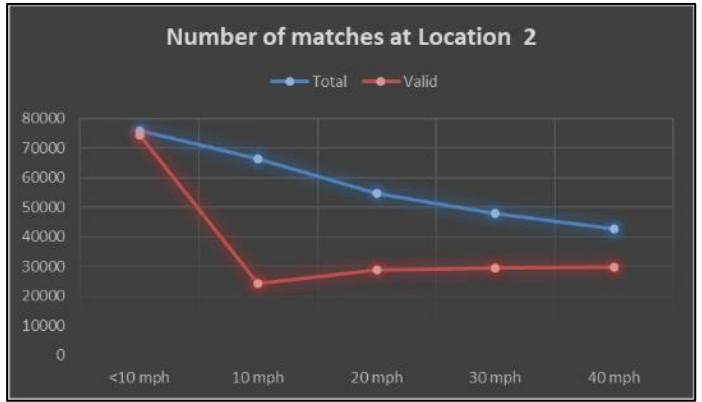


(c)



(d)

Figure 35 – (a-c) DJI M600 Drone with VX15 LiDAR Scanner. (d) DJI Mavic 2 Pro



(a)

(b)



(d)

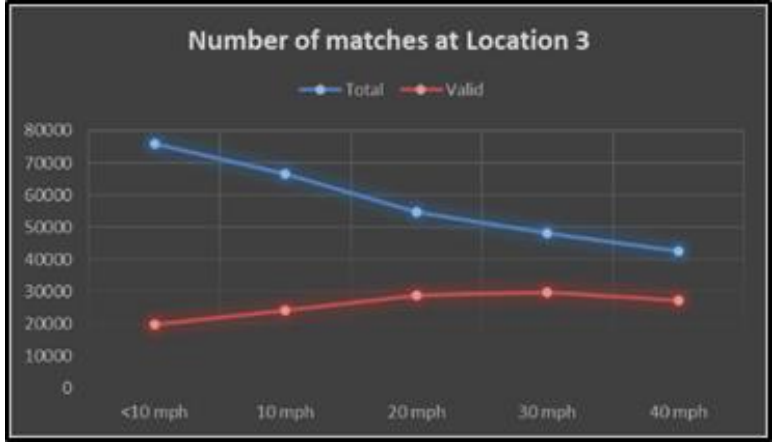
(e)



(g)

(h)

Figure 36 – Number of matches of keypoints at 3 locations. Images (a), (d), (g) are location 1. Images (b),(e),(h) are location 2. Images (c), (f), (i) are location 3.



(c)



(f)



(i)

Figure 36 cont.– Number of matches of keypoints at 3 locations. Images (a), (d), (g) are location 1. Images (b),(e),(h) are location 2. Images (c), (f), (i) are location 3.